AD-A099 121 SRI INTERNATIONAL MENLO PARK CA F/G 7/5
MECHANISMS OF MULTIPHOTON DISSOCIATION OF MOLECULAR IONS.(U)
APR 81 M J COGGIOLA, J R PETERSON, P C COSBY N00014-76-C-1035
UNCLASSIFIED SRI-MP-81-82 NL

1 OF 1
A
099121

END
DATE FILMED
8-81
DTIC

12

April 30, 1981

LEVEL

Final Report

MECHANISMS OF MULTIPHOTON DISSOCIATION OF MOLECULAR IONS

By: Michael J. Coggiola, Project Leader
James R. Peterson, Project Supervisor
Philip C. Cosby
Ronald V. Hodges

OFFICE OF NAVAL RESEARCH
800 North Quincy Street
Arlington, Virginia 22217

Contract No. N00014-76-C-1035
SRI Project No. PYU-5808

Approval:

D. C. Lorents, Director
Molecular Physics Laboratory

G. R. Abrahamson, Vice President
Physical Sciences Division

Approved for Public Release; Distribution Unlimited
MP 81-82

333 Ravenswood Ave. • Menlo Park, California 94025
(415) 326-6200 • Cable: SRI INTL MPK • TWX: 910-373-1246

SECURITY CLASSIFICATION OF THIS PAGE (When Date Entered)

REPORT DOCUMENTATION PAGE

READ INSTRUCTIONS BEFORE COMPLETING FORM

1. REPORT NUMBER: 6	2. GOVT ACCESSION NO.: AD-A099121
3. RECIPIENT'S CATALOG NUMBER:	
4. TITLE (and Subtitle): Mechanisms of Multiphoton Dissociation of Molecular Ions	5. TYPE OF REPORT & PERIOD COVERED: 9 Final Report, Sept 1976 — Mar 1981
	6. PERFORMING ORG. REPORT NUMBER: 14 SRI MP-81-82
7. AUTHOR(s): Michael J. Coggiola, Ronald V. Hodges, James R. Peterson, Phillip C. Cosby	8. CONTRACT OR GRANT NUMBER(s): N00014-76-C-1035
9. PERFORMING ORGANIZATION NAME AND ADDRESS: SRI International, 333 Ravenswood Avenue, Menlo Park, CA 94025	10. PROGRAM ELEMENT, PROJECT, TASK AREA & WORK UNIT NUMBERS: 11 61153N RR042-01
11. CONTROLLING OFFICE NAME AND ADDRESS: Office of Naval Research, Physics Program Office, Arlington, VA 22217	12. REPORT DATE: April 30, 1981
	13. NUMBER OF PAGES: 12 31
14. MONITORING AGENCY NAME & ADDRESS (if different from Controlling Office)	15. SECURITY CLASS. (of this report): Unclassified
	15a. DECLASSIFICATION/DOWNGRADING SCHEDULE

16. DISTRIBUTION STATEMENT (of this Report)

Approved for public release; distribution unlimited.

17. DISTRIBUTION STATEMENT (of the abstract entered in Block 20, if different from Report)

18. SUPPLEMENTARY NOTES

19. KEY WORDS (Continue on reverse side if necessary and identify by block number)

Multiphoton dissociation, polyatomic ions, infrared absorption, dissociation dynamics

20. ABSTRACT (Continue on reverse side if necessary and identify by block number)

The dissociation of highly vibrationally excited molecular ions resulting from single infrared photon absorption has been studied. The wavelength dependence of the absorption/dissociation process has been measured, and the photofragments identified. Measurements were also made of the dissociative lifetime following absorption and the photofragment kinetic energy distributions. These measurements show that a strong correlation exists between this single photon dissociation process and the final step of multiphoton dissociation. (see reverse)

DD FORM 1 JAN 73 1473 EDITION OF 1 NOV 65 IS OBSOLETE

SECURITY CLASSIFICATION OF THIS PAGE (When Date Entered)

Based on these results, the dissociation dynamics appear to follow a single statistical mechanism.

ACKNOWLEDGMENTS

The authors are grateful to the Office of Naval Research (ONR) for supporting this work and appreciate the interest and enthusiasm of Dr. B. R. Junker, the ONR technical monitor. They also appreciate the contributions of Dr. H. Helm and Professor R. C. Dunbar, who participated in some of the IR measurements and in their analysis.

INTRODUCTION

The research program supported by ONR under Contract N00014-76-C-1035 (SRI Project PYU-5808) has primarily been concerned with experimental studies of the mechanisms responsible for single and multiphoton dissociation (MPD) of molecular ions. With the development of intense lasers covering a wide range of wavelengths, multiphoton absorption and dissociation processes have become prominent research subjects because of their theoretical and applied importance. Yet, despite intensive study, little is known of the fundamental processes that govern these phenomena. Such information will have a strong impact on the future application of lasers to chemical processing, isotope separation, frequency conversion, and other military and nonmilitary applications important to our national security.

The work under this contract has focused on the transition between single and multiphoton absorption, which is believed to be the key step in initiating the multiphoton absorption in molecules in the presence of intense laser fields. Although multiphoton absorption and dissociation has been observed in numerous systems, the details of these initiating steps remain unknown. The influence of such variables as mass, charge, rotational state, and anisotropy in the molecular potential are also uncertain.

In addition to investigating this important transition region, we also extensively studied the final step in the multiphoton dissociation process, that is, the single photon dissociation of highly vibrationally excited molecular species. These studies probed the molecular regime often referred to as the "quasi-continuum." It has long been assumed that once a molecule reaches a sufficiently high level of vibrational excitation (either via the absorption of many IR quanta or some direct formation reaction), the density of states would essentially form a continuum. Under these conditions, any subsequent absorption process would be expected to be wavelength independent. This description received some early validation from several two-laser experiments where vibrationally excited molecules were found to undergo MPD at wavelengths removed from the ground state absorption bands. Nonetheless, it has also been suggested that the IR absorption strengths should remain peaked near

frequencies of the normal modes, even in the quasi-continuum. As a result of work done under this contract, the process of absorption and dissociation of molecular ions within the quasi-continuum has been significantly clarified.

Finally, this contract has also supported preliminary studies of the photoabsorption of the electronically excited atomic negative ion $He^-(^4P)$. This species, which is important in gaseous discharges and excited laser media, is weakly bound relative to the 2^3S metastable state of the neutral atom and thus has an excitation energy $\gtrsim$ 19.7 eV. Although this ion lies within the true continuum relative to He plus a free electron, it is metastable with respect to autodetachment and stable with respect to radiative decay. These unique properties make it possible to study the laser-induced photodetachment of He^-.

RESEARCH PROGRAM

A. Photodissociation

In the initial phase of the research program, we studied the infrared absorption spectrum of polyatomic molecular ions to obtain information on the vibrational states of these ions before studying the mechanisms of one- and two-photon absorption processes. The desired ions were formed in either a static dc discharge or via electron impact, then extracted, mass selected, and focused into a beam before they interacted with an IR laser beam. By merging the ion and laser beams colinearly over a 30-cm path and making use of the very high resolution wavelength tuning possible by velocity (Doppler) tuning the ion beam, we undertook preliminary studies of $^{16}O^{18}O^{+}$ and $^{16}O^{18}O^{-}$. We attempted to detect IR absorption in the positive ion case by observing changes in the fixed (visible) wavelength photodissociation yield as the IR wavelength was varied and in the negative ion case by observing corresponding changes in the photodetachment signal. Extensive searching produced no measurable evidence of an IR absorption in either O_2^{+}, O_2^{-}, or several other ions studied. It was subsequently found that these ions were produced in the source with very high degrees of vibrational excitation. As a result, it was not possible to drive transitions between levels that were essentially equally populated. Further investigation showed that, in fact, these ion species were sufficiently excited so that they could be dissociated using a single infrared photon of energy $< 1000\ cm^{-1}$; that is, the ions were produced initially in very high vibrational states, and electronic transitions to repulsive states were excited at IR wavelengths. This fact was confirmed by using $^{16}O_2^{+}$, which has no purely vibrational electronic moments, but which was nevertheless photodissociated by the IR laser. No significant wavelength dependence was observed, which was consistent with our interpretation.

As a result of this discovery, we began a systematic study of the single IR photon dissociation of highly vibrationally excited molecular ions. In addition to measuring the wavelength dependence of the IR photodissociation of excited molecular ions, we were also able to measure the translational energy release accompanying dissociation, as well as the dissociative lifetime of ions following absorption.

Table 1 lists the ions studied and the type of information measured for each. More complete and detailed reports of the photodissociation of CF_3I^+, CF_3Br^+, and CF_3Cl^+ have also been published and are included in Appendices A and B. A full description of the relevant experimental methods used in measuring both the wavelength dependence and the translational energy spectra is given therein.

As shown in Table 1, many of the ions studied could be readily photodissociated by a single IR photon from a low-power CO_2 laser. Interestingly, the yield of photofragments was often a strong function of wavelength. For example, the dissociation cross section of CF_3I^+ peaked sharply at 947 cm^{-1} (see Figure 1, Appendix A). The strong wavelength dependence for absorption of this and other highly vibrationally excited molecular ions is one of the most significant results of our work, and its interpretation is discussed at length in Appendix A. It suffices to say here that these absorption features result from the excitation of one of the fundamental vibrational modes of the ion. Thus, even though the ion is highly excited and lies well within the quasi-continuum, its absorption strength tends to remain peaked at characteristic frequencies. This rather unexpected result has allowed us to identify for the first time the ν_1 C-F symmetric stretch frequency in several ions. In fact, in each ion studied to date, the absorption can be atributed to a C-F, stretching mode with a frequency of ~ 1000 cm^{-1}. Thus, attempts to photodissociate CH_3I^+ proved unsuccessful because no appropriate vibrational mode falls within the tuning range of the CO_2 laser. Additional examples of the wavelength dependence of the ion photodissociation yield are given in Figures 1 through 5 for a variety of species. In each case, the dissociation yield shows distinct peaking about a wavelength in the 900 to 1100 cm^{-1} region.

As a result of the unique features of the laser-ion coaxial beams spectrometer used in this work, we were able to obtain an approximate estimate of the dissociation lifetimes of several longer lived ions excited by the low-power laser. This measurement was accomplished by observing the photofragment signal produced over two different path lengths. Knowing the ion velocity and the two flight lengths, we can use the measured signals to deduce the dissociation lifetime. The measured lifetimes for four ions of varying complexity are listed in Table 1. For each of these ions, we also observed a metastable

Table 1

SUMMARY OF ION SYSTEMS STUDIED

ION	PRODUCT ION	WAVELENGTH DEPENDENCE	ENERGY RELEASE IR (meV)	ENERGY RELEASE CID (meV)	LIFETIME (μsec) IR	LIFETIME (μsec) META
CF_3I^+	CF_3^+	p 947	4.4	1.3	-	-
CF_3Br^+	CF_3^+	p 953	3.8	-	-	-
CF_3Cl^+	CF_3^+	b	-	-	-	-
$C_2F_5I^+$	$C_2F_5^+$	p 1080	10.0	2.0*	1.7	7.4
$C_2F_5Br^+$	$C_2F_5^+$	p 1080	8.0	-	-	-
$C_3F_7I^+$	$C_3F_7^+$	p 1000	14.0	10.1*	6.6	29.2
$C_3F_6^+$	$C_2F_4^+$	p 1030	13.4	11.6*	2.8	11.7
CF_2I^+	I^+	b	10	-	-	-
CF_3^+	CF_2^+	-	-	-	-	-
CH_3F^+	CH_2F^+	b	14	10	-	-
CH_4F^+	CH_3F^+	-	1	1	-	-
$C_2F_5^+$	CF_3^+	p 1035	14	8	-	-
$C_6F_6^+$	$C_5F_3^+$	b	-	130*	-	-
$C_6F_5I^+$	$C_6F_5^+$	b	-	49*	14.6	45.2
$C_6F_5Br^+$	$C_6F_5^+$	-	-	96*	-	-
$C_6F_5Cl^+$	$C_6F_5^+$	-	-	69*	-	-

p = peak; b = broad; - = not measured; * = metastable

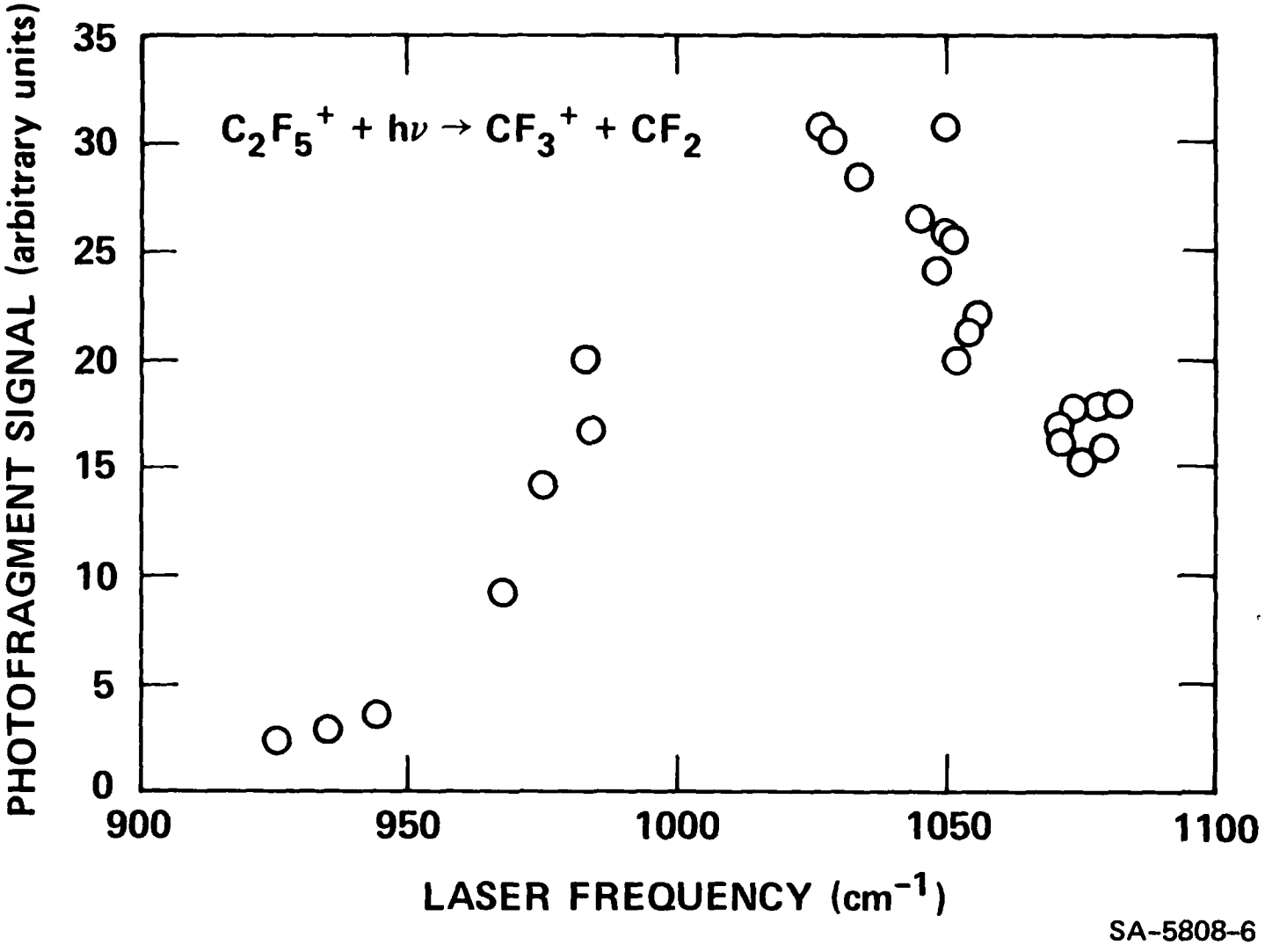

FIGURE 1 PHOTODISSOCIATION YIELD OF $C_2F_5^+$ AS A FUNCTION OF IR LASER FREQUENCY, CORRECTED FOR INCIDENT POWER VARIATIONS

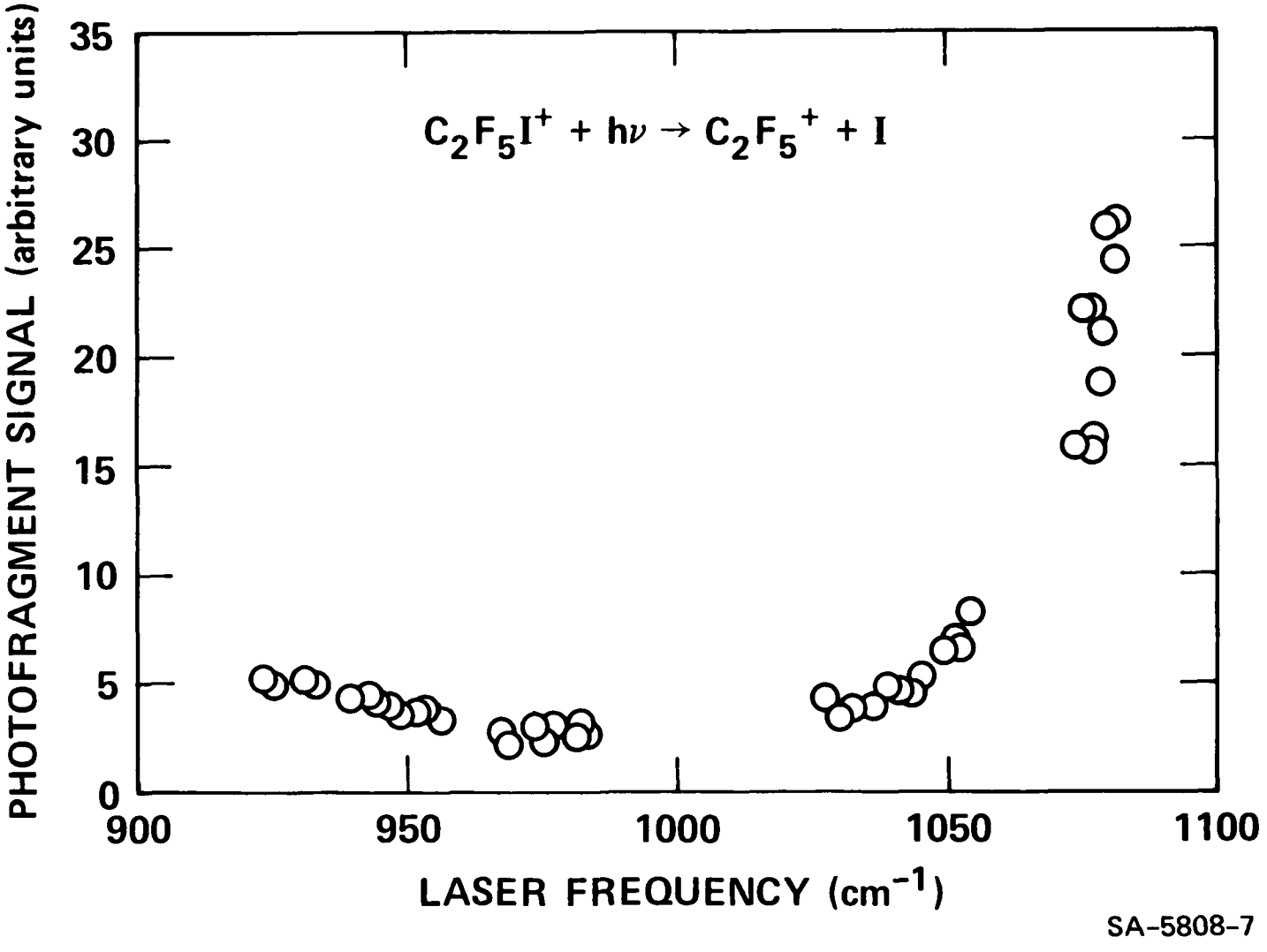

FIGURE 2 PHOTODISSOCIATION OF $C_2F_5I^+$

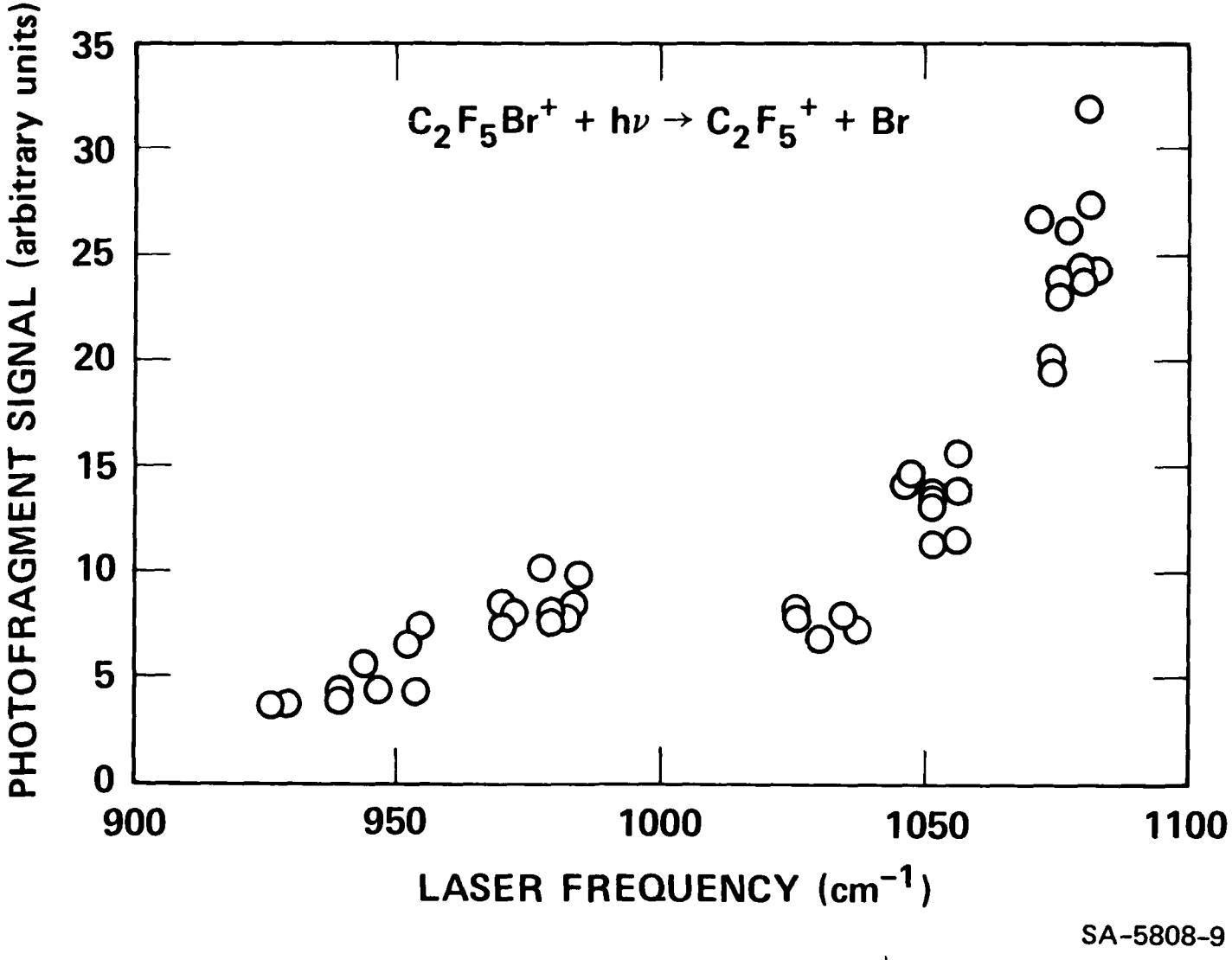

FIGURE 3 PHOTODISSOCIATION OF $C_2F_5Br^+$

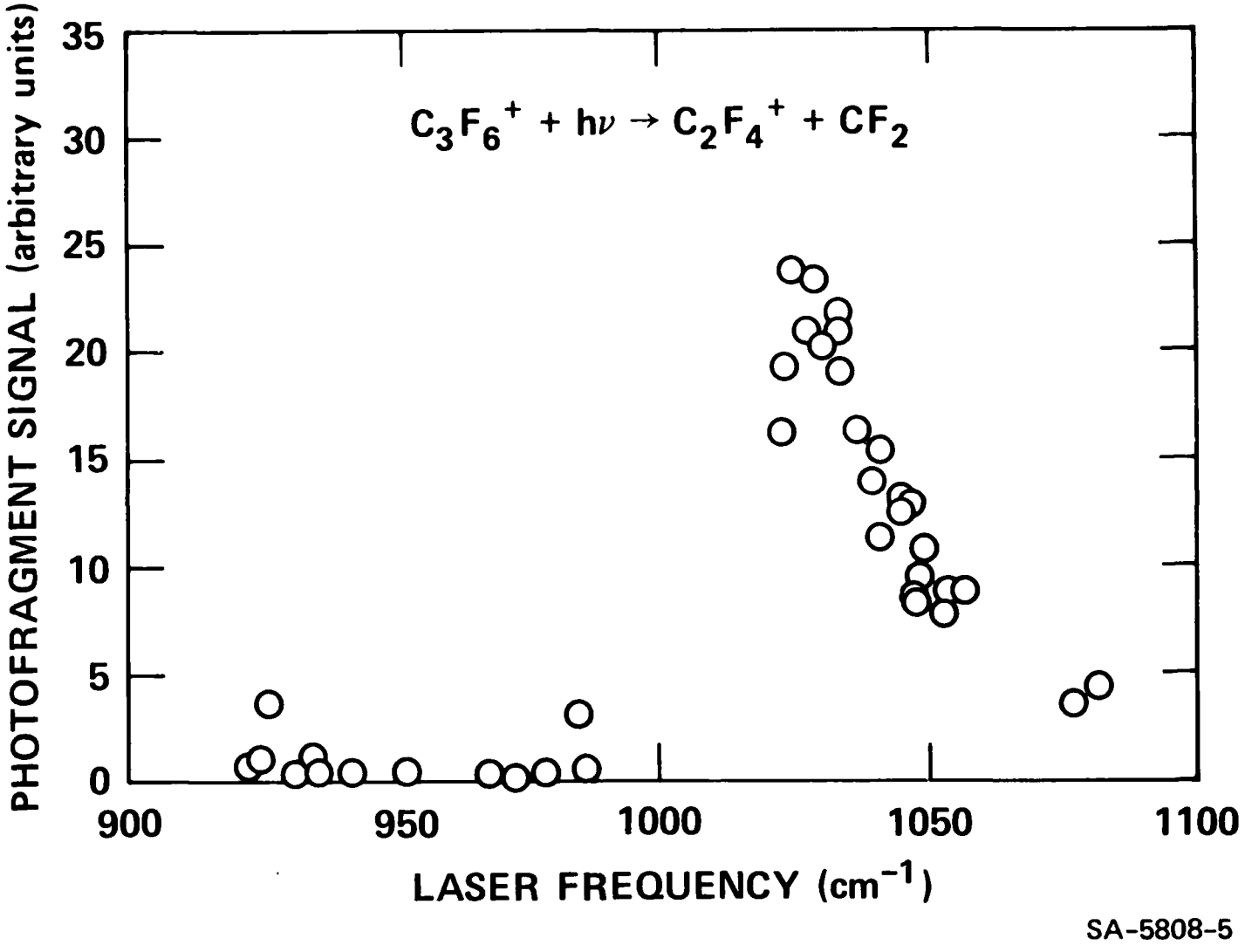

FIGURE 4 PHOTODISSOCIATION OF $C_3F_6^+$

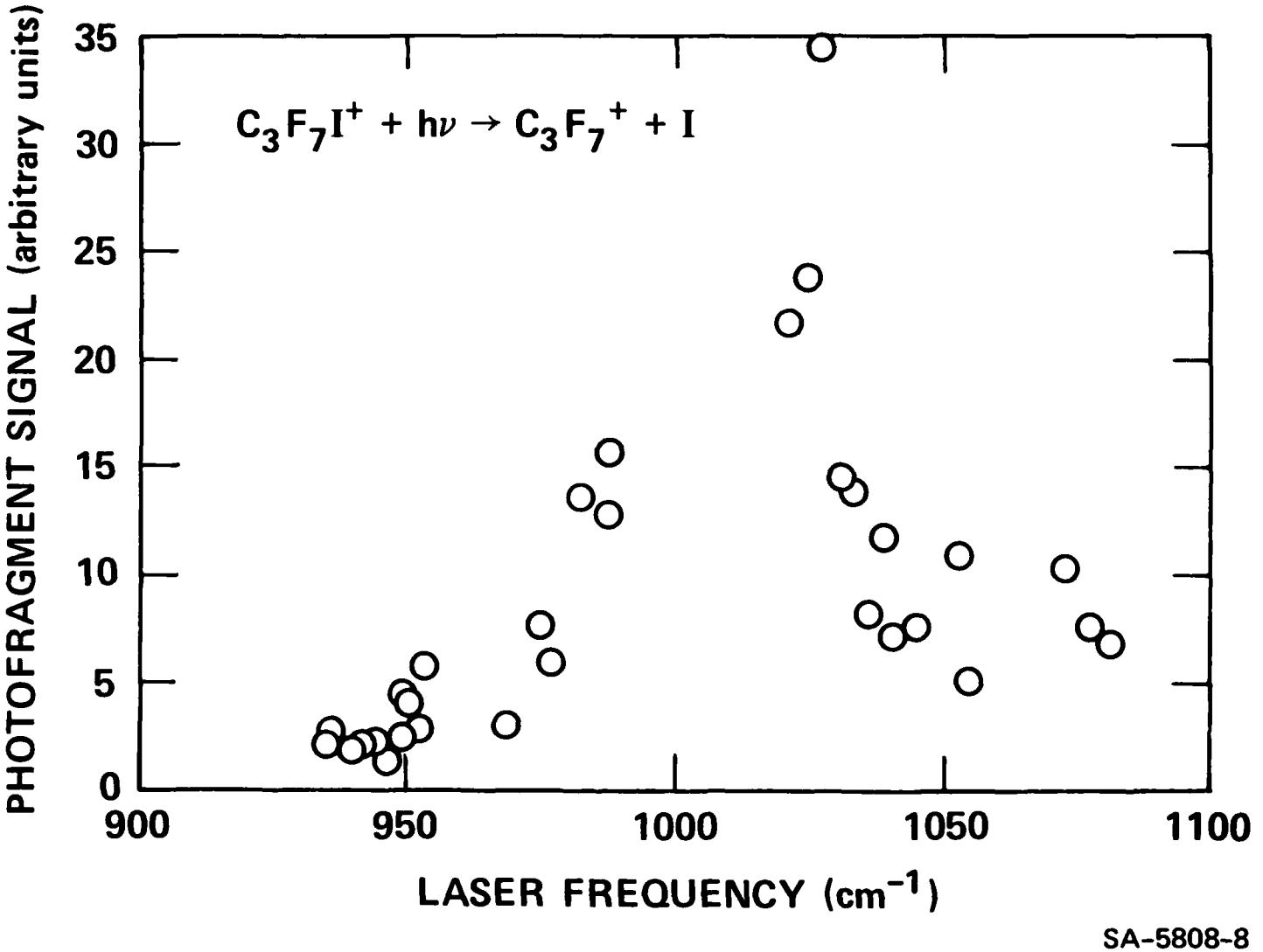

FIGURE 5 PHOTODISSOCIATION OF $C_3F_7I^+$

component in the beam giving rise to a fragment signal in the absence of the laser. These metastable ions must necessarily be produced in the source with a total internal energy exceeding the dissociation limit. The lifetimes of these metastable ions were measured in the same way as the photoexcited ions and are included in Table 1.

Two trends can be seen in these results. First, the photodissociation lifetimes are in each case significantly shorter than the corresponding metastable lifetime. Second, the lifetimes increase with increasing molecular complexity. Both of these characteristics may be rationalized by invoking several features of the well-known RRKM theory of unimolecular decomposition, which has proven to be applicable in MPD. Specifically, the relationship between the photodissociation lifetime and the metastable lifetime for a given ion reflects the amount of excess energy present in each case. The observed ordering of the lifetimes implies that the average $E^{\ddagger}$ ($= E_{total} - E_{dissoc}$) of the metastable ions is less than the average of ions that have absorbed infrared radiation. As a consequence, one would expect to measure a correspondingly smaller kinetic energy release in the metastable dissociation process as compared with the photodissociation process. This behavior has in fact, been observed for the $C_2F_5I^+$ ions. The variation of the lifetime with molecular complexity is consistent with the RRKM view of energy partitioning among all vibrational modes. In this view, the total internal energy is distributed randomly among all the vibrational modes, and the molecule will only dissociate when enough energy becomes localized in the proper nuclear motion. In principle, the lowest energy channel will always provide the first opportunity. The larger the molecule, the longer will be the lifetime, provided the system behaves ergodically.

These results have provided the first real information on the nature of infrared absorption processes in the quasi-continuum and the subsequent dissociation of the molecular ions. Several important trends have thus far been identified from these results on the absorption spectra, fragment kinetic energy release, and dissociative lifetimes. This work has also provided information on energy redistribution in highly excited ions, variations in the absorption cross section and dissociative lifetime as a function of molecular complexity, and the identification of IR active vibrational modes.

B. Photodetachment

In addition to the photodissociation work described above, this ONR contract also supported a preliminary experimental investigation of the photodetachment of the highly excited negative ion of He. Using a different atomic beam apparatus, we investigated both the wavelength dependence and the absolute magnitude of the He^- photodetachment cross section. A complete report of this work is given in Appendices C and D.

The results of this photodetachment study are clearly preliminary; however, they have already stimulated renewed theoretical interest in this important metastable negative ion. Because He^- is produced in a variety of excited laser media, discharges, and other energy transfer/ionization media and probably in other stellar atmospheres, these initial studies should prove useful in furthering the understanding of these areas.

APPENDIX A

Infrared photodissociation of polyatomic ions

M. J. Coggiola, P. C. Cosby, and J. R. Peterson

Molecular Physics Laboratory, SRI International, Menlo Park, California 94025
(Received 15 January 1980; accepted 27 February 1980)

Dissociation of CF_3I^+, CF_3Br^+, and CF_3Cl^+ ions resulting from the absorption of a single 10 μ IR photon by highly vibrationally excited parent ions under collision-free conditions is reported. In each case, the only observed products are $CF_3^+ + X$. Dissociation yields as a function of photon wavelength for CF_3I^+ and CF_3Br^+ peak sharply at ~ 950 cm^{-1} corresponding to a strong absorption frequency in the molecular ion. Product ion translational energy distributions are measured for CF_3I^+ and CF_3Br^+ photodissociation, and indicate that the energy release is $\ll h\nu$. The observed dissociation can be interpreted as resulting from the unimolecular decomposition of ions, initially formed with a total energy within 900–1000 cm^{-1} of the dissociation limit, that absorb a single infrared photon. Thus, this process corresponds directly to the final step in IR multiphoton dissociation of polyatomic ions.

I. INTRODUCTION

In the last five years substantial theoretical and experimental efforts have been devoted to studies of infrared multiphoton excitation (MPE) and dissociation (MPD) of polyatomic molecules. Out of this work, a qualitative model has evolved which gives a reasonable explanation for the general characteristics of the experimental results but which is largely semiempirical with some aspects not clearly understood. Reviews of both the experimental work and the model have been given by Bloembergen and Yablonovitch[1] and by Schulz *et al.*[2] It is usually assumed that both MPE and MPD in polyatomic molecules can be characterized by two different stages. First is the stepwise absorption of perhaps a few photons which excite successive discrete levels of a single vibrational mode. Any red shifts due to vibrational anharmonicities can be accommodated by power broadening. However, after some number (which depends on the molecule) of photons have been absorbed, the density of states of the other initially unexcited normal modes at this total energy is assumed to form a quasicontinuum (QC) and any further energy absorbed is rapidly redistributed among these other modes. This energy redistribution among all other modes is found to be statistical, and when a sufficient number of photons have been absorbed, such that the total internal energy exceeds the dissociation limit, the molecule may undergo unimolecular decomposition. This last step can be described by the RRKM theory[3] of unimolecular reactions.

One of the open questions of this model concerns the characteristics (strength and frequency dependence) of the absorption spectrum of highly vibrationally excited molecules. From the results of some MPD experiments, and from theoretical arguments it appears that the absorption profile in this regime is considerably broader than for the first few discrete absorptions, and it is nonzero at frequencies far from the original resonance. However, it has also been argued[1] that some resonance characteristics may still exist even at high levels of excitation where the density of states is exceedingly large.

Our experiment was originally designed to make use of the excellent sub-Doppler resolution obtainable in our coaxial laser–ion beam spectrometer[4] to determine details of the first few IR (discrete) absorptions in MPE of molecular ions. However, these studies were precluded by a highly vibrationally excited parent ion beam which has instead made possible some unique studies of the photoabsorption spectra of such ions.

Recently, infrared multiphoton dissociation (MPD) of molecular ions has been studied in ICR spectrometers utilizing both a low power cw CO_2 laser[5] and a high power pulsed TEA CO_2 laser,[6] as well as in a crossed beam experiment with a pulsed laser.[7] In these experiments, the MPD of several polyatomic molecular ions was observed under essentially collision free conditions. In the first case, ions were continuously irradiated for periods of up to 1 sec in an ICR ion trap with the yield of product ions determined directly. For some ions, the yield was found to be a sensitive function of the excitation wavelength. For example, the yield of $C_2F_4^+$ from the MPD of perfluoropropylene ($C_3F_6^+$) as a function of laser wavelength matched very closely the infrared absorption profile of the C–F stretch in the neutral C_3F_6 molecule.

In the present study, we have observed the photodissociation of CF_3I^+, CF_3Br^+, and CF_3Cl^+ in a fast ion beam using a low power cw CO_2 laser. The dissociation appears to result from a single photon absorption by highly vibrationally excited ions that exist in the beam The results can be interpreted in terms of these absorptions corresponding to the final step in a low power IR multiphoton dissociation process. In this respect, the results offer unique information on MPD processes. The single photon mechanism is supported by the linear power dependence of the dissociation signal, as well as by a consideration of the laser flux and interaction time. The identities of the fragment ions were determined along with their relative yield as a function of laser wavelength. In addition, the center of mass recoil energy distributions of the photofragments were directly determined for the CF_3I^+ and CF_3Br^+ cases. The translational energy release is found to be $\ll h\nu$ and is consistent with the single photon dissociation mechanism.

II. EXPERIMENTAL

The laser–ion coaxial beams spectrometer used in this work has been described in detail elsewhere,[4] and has been used extensively for photofragment spectros-

 0021-9606/80/126507-06$01.00

copy of diatomic ions.[8] Briefly, ions formed in the pure parent gas by electron impact at 100 eV are extracted and accelerated to a final kinetic energy of 2.5 keV. The production of ions with high levels of internal excitation is well known in electron impact sources of the type used here.[9] An indication of this degree of excitation is seen in the collision-induced dissociation (CID) signal, which is observed in the differentially pumped interaction region at pressures of 5×10^{-8} Torr. The mass selected ion beam was electrostatically deflected by 90° and merged with the unfocused output from a line tunable Advanced Kinetics MIRL-50 CO_2 laser. The laser light was collimated to 3 mm diameter and overlapped the ion beam for a distance of ~ 33 cm before the fragment ions were deflected 90° by an electric field. The transmitted laser power was typically 0.5–1.0 W at $P(16)$ in a TEM_{00} mode, although the power in the interaction region was likely 2–3 times higher. The laser wavelength was determined using a grating spectrum analyzer. The kinetic energies of fragment ions were determined using a 180° hemispherical electrostatic analyzer. From the measured laboratory kinetic energy distribution of the product ions, it is possible to deduce the center of mass energy release that accompanies the photodissociation process.[4] In addition, this energy analysis serves to identify uniquely the masses of the fragment ions. Since the fragment ions produced by photodissociation were

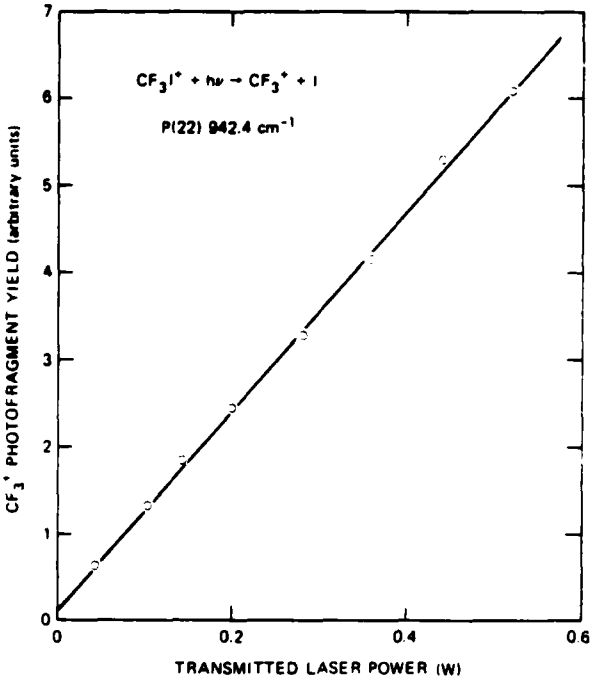

FIG. 2. Power dependence of CF_3I^+ photodissociation at 942.4 cm^{-1}, $P(22)$.

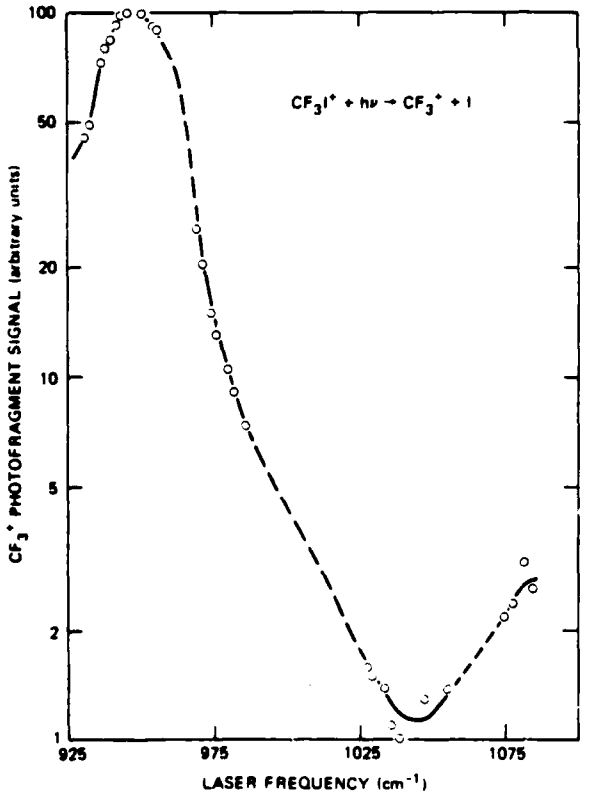

FIG. 1. Frequency dependence of the CF_3^+ fragment yield from CF_3I^+ corrected for laser power variations. Dashed line indicates CO_2 laser tuning gaps.

the same as those produced by CID, it was necessary to modulate the photon beam and to use single particle lock-in detection methods to discriminate against this background.

The interaction region of the apparatus includes an electrostatic cage, which can be used to perform high resolution Doppler-tuned experiments. For this type of measurement, the single mode output frequency of the laser was actively stabilized to the peak of one CO_2 line gain profile. By sweeping the cage voltage ± 250 V about ground potential, a frequency shift of ± 145 MHz could be produced in CF_3I^+. The estimated overall width of the laser line and the residual Doppler width of the CF_3I^+ beam was ≈ 1 MHz.

III. RESULTS AND DISCUSSION

Figure 1 shows the yield of CF_3^+ fragment ions produced by the photodissociation of CF_3I^+ parent ions as a function of the CO_2 laser frequency. The fragment ion intensities have been corrected for the transmitted laser power at each wavelength. The data clearly show a strong maximum in the photodissociation probability centered at about 947 cm^{-1}, with a FWHM of ~ 30 cm^{-1}. In addition, a distinct but smaller absorption feature is reproducibly found at about 1080 cm^{-1}. Between the absorption maxima, the fragment ion yield drops to about 1% of its peak value. The power dependence of the CF_3^+ photofragment ion signal near the peak absorption is shown in Fig. 2, for transmitted powers between 0.05 and 0.52 W at 942 cm^{-1} [$P(22)$ line]. Over this range of laser power, no significant deviation from a linear dependence was observed. Additional studies

made using a weakly focused laser beam extended this linear measurement to ~3 W transmitted power. Figure 3 presents the CF_3^+ photofragment recoil energy distribution measured with a photon wavelength of 975 cm^{-1} [$R(20)$ line]. Also shown for comparison in Fig. 3 is the recoil energy distribution for CID fragments. The angular discrimination of the apparatus[4] leads to the preferential detection of ions with small recoil energies. However, over the relatively small range of energies measured here (0–20 meV), the correction is small and increases the FWHM of the distribution by at most 10%–20%. Therefore, this correction has not been applied to the data in Fig. 3. Thus, it is seen that under the present conditions, photofragments are produced with an average of only 4.4 meV of translational energy and a maximum of ~ 100 meV. In contrast, the CF_3^+ fragments produced by CID have a significantly narrower energy distribution with an average energy release of 1.2 meV. The CF_3^+ photofragment kinetic energy distribution was measured using several other CO_2 laser lines on both sides of the main absorption feature, and were quantitatively equivalent to that shown in Fig. 3.

The effect of source electron energy on the CF_3I^+ photofragment yield at the absorption peak was also studied. It was possible to reduce the nominal electron energy to within a few volts of the 10.23 eV I.P. of CF_3I[10] and still produce useable CF_3I^+ beam currents (1×10^{-14} A) and measurable CF_3^+ photofragment count rates. Under these conditions, the fractional yield of CF_3^+ photofragments was found to be independent of electron impact energies between 100 eV and near threshold.

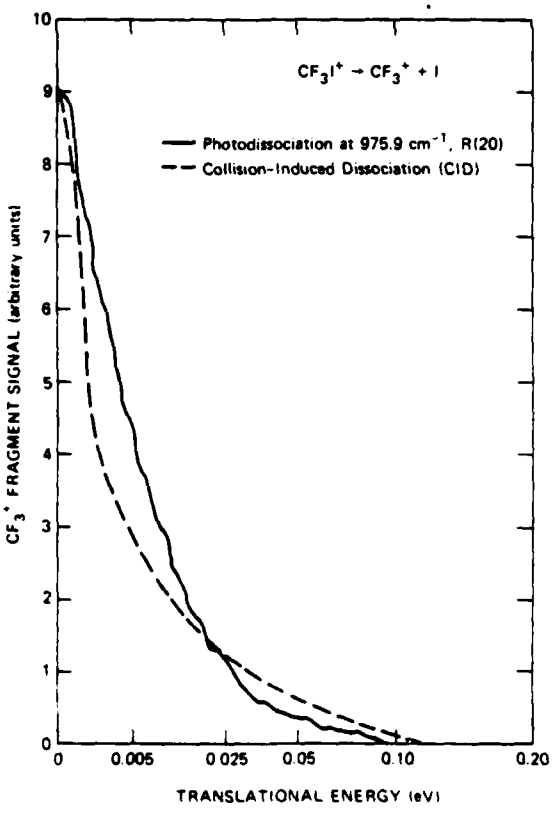

FIG. 3. Center of mass kinetic energy release for CF_3^+ fragments produced from CF_3I^+.

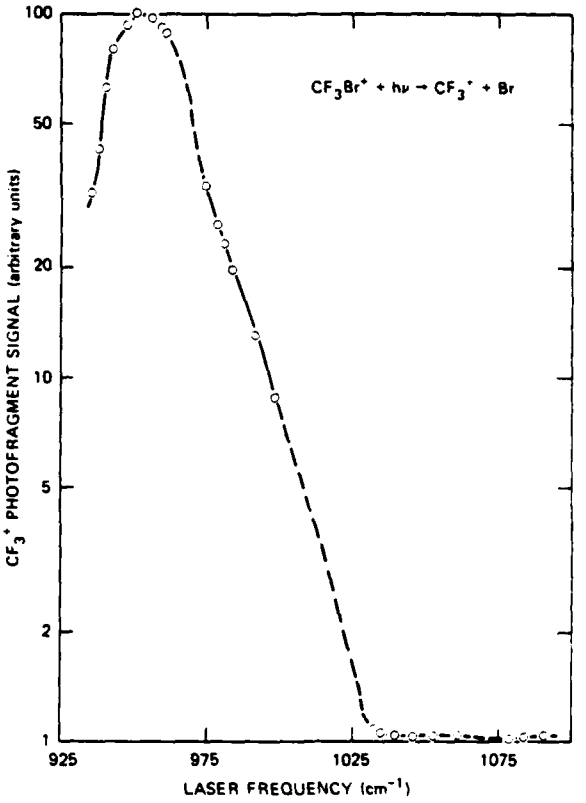

FIG. 4. Frequency dependence of CF_3^+ fragment yield from CF_3Br^+ corrected for laser power variations. Dashed line indicates CO_2 laser tuning gaps.

Figure 4 shows the wavelength dependence for CF_3^+ produced from the infrared photodissociation of CF_3Br^+ ions. The mass resolution of the apparatus allowed the ^{79}Br and ^{81}Br isotopic species to be studied separately. To within the experimental uncertainty, the results were the same. The wavelength dependence of the CF_3Br^+ photodissociation shows a strong maximum centered at about 953 cm^{-1} with a FWHM of ~ 30 cm^{-1}. This absorption peak is very similar to the major CF_3I^+ peak, both in location and width. Here, however, no additional absorption feature is found in the 1050–1100 cm^{-1} region. We note, however, that away from the absorption maximum, the yield remains nearly constant at ~ 1% of the peak value. The power dependence was again found to be linear between 0.04 and 0.5 W transmitted power. The measured CF_3^+ photofragment kinetic energy distribution has a width of 3.8 meV with a shape qualitatively the same as that found in the CF_3I^+ case. The effective photodissociation cross section of CF_3Br^+ was approximately 90% of that measured for CF_3I^+ under similar conditions.

A brief study was also made of the infrared photodis-

TABLE I. CF_3X^+ bond dissociation energies.[a]

Dissociation channel	Endoergicity (eV) X = Cl	X = Br	X = I
$CF_3X^+ \rightarrow CF_3^+ + X$	0.6	0.5	1.3
$CF_3 + X^+$	4.1	2.8	2.5
$CF_2^+ + FX$	4.1	3.9	4.3
$CF_2 + FX^+$	5.0	4.0	3.1

[a] Data from Ref. 11.

sociation of CF_3Cl^+ ions. Production of CF_3^+ photofragments was observed at photon energies between 931–1048 cm^{-1} with an apparent cross section of $4 \pm 2 \times 10^{-21}$ cm^2. In contrast to CF_3I^+ and CF_3Br^+, whose photodissociation cross sections vary by nearly 2 orders of magnitude over this photon energy range, variations in the CF_3Cl^+ cross section are less than a factor of 2 and were, in all cases, within the standard deviation of the measurements. Because of very small CF_3Cl^+ beam currents (1% of CF_3I^+), no laser power dependence or photofragment kinetic energy spectra were taken of this ion.

For each ion studied, the observed photodissociation process yields only CF_3^+ ions, corresponding to

$$CF_3X^+ + h\nu \rightarrow CF_3^+ + X, \quad (1)$$

$$X = Cl,\ Br,\ I.$$

On the basis of the detection limits, we conclude that alternative channels, such as

$$CF_3X^+ + h\nu \rightarrow CF_3 + X^+ \quad (2)$$

$$\rightarrow CF_2^+ + FX \quad (3)$$

$$\rightarrow CF_2 + FX^+, \quad (4)$$

must contribute less than 1% to the total photodissociation cross section. As shown in Table I, the observed dissociation channel corresponds in each case to the least endothermic process.[11]

Although it may not be possible to establish the exact photodissociation mechanism from this work alone, several major features are evident and point toward some interesting conclusions. Under the present conditions, ions remain in the interaction region for 6–8 μsec where the typical photon flux is $1-5 \times 10^{21}$ sec^{-1} cm^{-2}. For any reasonable infrared absorption cross section ($\sigma < 10^{-17}$ cm^2), the probability that an ion will absorb more than a single infrared photon is very small. For $\sigma = 10^{-17}$ cm^2 the probability of a single absorption is ~ 0.2, whereas the two-photon absorption probability is more than 1 order of magnitude less. It is thus reasonable to conclude that the observed dissociation arises from a single photon absorption process, with the implication that only those ions with a total internal energy content that is within $h\nu$ (0.12 eV) of the dissociation limit can contribute to the observed process. The measured linear power dependence is consistent with a single photon absorption. The small kinetic energy release observed here ($\ll h\nu$) is also supportive of a single photon mechanism because in pulsed laser multiphoton studies (at fluxes of ~ 10^{29} sec^{-1} cm^{-2}) of the corresponding CF_3X neutral species[12] the average energy release is found to be $> h\nu$.

In view of the proposed single photon dissociation mechanism, the strong wavelength dependence shown in Figs. 1 and 3 is at first unexpected because photons of any wavelength in the 1000 cm^{-1} region should be energetically capable of producing dissociation. This resonant behavior may be explained, however, if one assumes that the total internal energy that must be present in the ions before absorption is statistically partitioned among the nine fundamental vibrational modes, as is generally assumed in models of unimolecular dissociation[3] and MPD.[1,13] In that case, each mode would, on the average, contain less than one quantum of excitation. The absorption process would then correspond approximately to the $0-1$ or $1-2$ transition of one of the fundamental modes of the CF_3X^+ molecular ions. In the neutral CF_3I molecule, the mode closest to the observed 947 cm^{-1} absorption in the CF_3I^+ ion is the C–F symmetric stretch ν_1 mode, which occurs at approximately 1073 cm^{-1}.[14] Assigning the 947 cm^{-1} feature to the ν_1 absorption mode of the ion would imply that ionization leads to a weakening of the C–F bonds and hence to a decrease in the bond-stretching constant. Strong support for this behavior can be found from a far ultraviolet absorption study of CF_3I where the vibrational spacings in at least one member of a Rydberg series leading to the ion were measured.[15] It was found that the ν_1 mode vibrational spacing in the $7s\sigma$ Rydberg state (8.76 eV) was ~ 950 cm^{-1}. It is not unreasonable to assume that such high lying Rydberg states are closely related to the corresponding ion, which is formed by removal of the Rydberg electron. It therefore appears likely that the main feature observed in Fig. 1 at 947 cm^{-1} is due to the ν_1 C–F stretch absorption in CF_3I^+.

Following absorption, some ions will contain sufficient total energy to dissociate and hence will undergo unimolecular decomposition with a characteristic rate. As long as this characteristic lifetime (= 1/rate) is shorter than the average ion transit time between the point of absorption and the deflection of the fragment ions before detection (~ 3 μsec), the overall process will appear to be simple photodissociation [Eq. (1)].

It was possible to determine an "apparent" cross section for the photodissociation of CF_3I^+ by measuring both the current of CF_3^+ fragments and the CF_3I^+ parent ion beam at the exit of the interaction region. A major uncertainty in determining the cross section was in the estimation of the actual laser power density in the overlap region. Lacking any direct observation, we have assumed that this power density was twice the measured power transmitted through the apparatus. The resulting apparent cross section (σ_{app}) determined at the absorption peak is 3.7×10^{-20} cm^2. Note that this cross section is an average over all of the internal energy levels populated in the beam. If, however, only a small fraction of the beam molecules contain sufficient

internal energies to be dissociated by a single photon, then the cross section would be correspondingly larger.

Considering this problem from a different viewpoint, if the photoabsorption cross section of those molecules whose internal energies lie within $h\nu$ of the dissociation limit were known, then we could determine the percentage of the beam population that they constitute. It is reasonable to assume that the oscillator strength for the C–F stretch mode in the ion is roughly the same as for the neutral, and that the shape of the absorption cross section we observe represents the envelope of the *P*, *Q*, and *R* branches, smoothed out by the excitation and broadened by the effects of the redistribution rate in the quasicontinuum. We can then use the absorption spectra and effective absorption strengths observed in the neutral CF_3I to determine the transition rate, A, for the C–F stretch absorption in CF_3I^+, which can then be used to obtain the peak absorption cross sections as $\sigma = \lambda^2 A/8\pi c\Delta\nu$. From the data of Plyler and Acquista,[16] we estimate $A = 220\ \text{sec}^{-1}$, and from the data of Jones and Kohler,[17] we estimate $A = 150\ \text{sec}^{-1}$. We thus chose $A = 180\ \text{sec}^{-1}$, and using our observed $\Delta\nu$ of 30 cm^{-1}, we find $\sigma_{max} = 9\times10^{-18}\ \text{cm}^2$. This value, compared with our observed σ_{app} of $3.7\times10^{-20}\ \text{cm}^2$, implies that about 0.4% of the CF_3I^+ ions in the interaction region contain total internal energy within $h\nu$ of the dissociation limit.

It is worth noting that these ions have traveled for about 25 μsec after leaving the ion source before reaching the interaction region. Although we observed no spontaneous dissociation due to metastable CF_3X^+ molecular ions in the beam that reaches the interaction region, we have observed such decay in larger ions, whose unimolecular dissociation rates are slower.[3] Thus, some small fraction of all ions produced in our source probably contain energies above the dissociation limit and hence can dissociate before reaching the interaction region depending on their decay rates. However, the only mechanism for energy loss below the dissociation limit is radiation, which is very slow compared with the observation time in this experiment.

Considering the magnitude of the ν_1 frequency shift between the neutral CF_3I and the ion, the smaller secondary feature seen at ~ 1080 cm^{-1} in Fig. 1 may be tentatively assigned as the ν_4 antisymmetric C–F stretch of CF_3I^+ [$\nu_4(CF_3I) = 1185\ \text{cm}^{-1}$]. No support for this assignment can be obtained from the far UV absorption studies, however, because the ν_4 mode was not observed. The neutral CF_3Br has a ν_1 frequency of 1082 cm^{-1}, and so it is not unexpected that the ν_1 mode of the ion will also shift to the 950 cm^{-1} region. The strong peak found in Fig. 4 can therefore be associated with the ν_1 absorption of CF_3Br^+. The ν_4 mode of CF_3Br at 1207 cm^{-1} might also have been expected to shift to the 1080 cm^{-1} region as in the CF_3I^+ case. However, a larger (or smaller) frequency shift between the neutral and the ion or a narrow absorption feature that falls within one of the tuning gaps of the CO_2 laser branches could explain its absence.

As noted earlier, σ_{app} for CF_3Cl^+ does not change appreciably with wavelength over the 930–1090 cm^{-1} tuning range of the CO_2 laser. Here, the ν_1 mode of the neutral is 1106 cm^{-1} so that the ion absorption is expected to occur within this range. Of course, the frequency shift between the neutral and the ion may be larger (or smaller) than those observed for CF_3I^+ or CF_3Br^+, so that the CF_3Cl^+ absorption maximum falls outside the limited tuning range of the laser. The value we measure for σ_{app} of CF_3Cl^+, however, is a factor of 10 larger than those we measure for the other halides when the laser is tuned away from their absorption maxima. Nevertheless, the actual photodissociation cross section may be comparable to those of CF_3I^+ and CF_3Br^+ if a significantly larger fraction of the CF_3Cl^+ beam participates in the photodissociation, that is, if it has a total internal energy within one photon of the dissociation limit. There is reason to suspect that this may be the case.

The appearance potentials of CF_3X^+ and CF_3^+ have been reported[10] for both CF_3Cl and CF_3I. The difference between the appearance potentials of the two product ions gives a lower limit to the internal energy with which the CF_3X^+ ion is formed at its threshold, relative to the CF_3^+–X dissociation limit. For CF_3I, this difference is 0.56 eV, which contrasts with the threshold formation of CF_3Cl^+ only 0.14 eV below its dissociation limit.

It is reasonable to expect that at the high electron impact energies used in the present experiment, the CF_3Cl^+ will be produced with the same or higher degree of internal excitation. This is also supported by our observation that the current of CF_3Cl^+ ions was nearly 2 orders of magnitude smaller than either CF_3I^+ or CF_3Br^+. This implies that a significantly larger fraction of CF_3Cl^+ ions are formed with total internal energies greater than the dissociation energy and are thus removed from the beam by unimolecular decomposition. One would also expect that of the ions which survive the trip from the source to the photon interaction region, a larger fraction will have internal energies within one photon of the dissociation limit, thus contributing to their larger apparent photodissociation cross section.

A preliminary survey has shown that a variety of molecular ions can be photodissociated in our apparatus using only a single infrared photon. For example, CH_2F^+, CH_2F^+, $C_2F_5I^+$, and $C_3F_7I^+$ are all dissociated using the low power CO_2 laser.[18] In contrast, CH_3I^+ produced under similar conditions to the CF_3I^+ showed no detectable photodissociation at power densities up to 40 W/cm^2. It thus appears that a vibrational mode of the appropriate frequency (such as the ν_1 symmetric stretch in CF_3X^+) is necessary to achieve single IR photon dissociation. Hence, the C–F stretch in each of the dissociated ions provides the required absorption mode whereas the corresponding C–H vibration in CH_3I^+ lies outside the present frequency range.

The observed photodissociation process is related to the MPD of both ions and neutrals in several respects. In each case, the molecule absorbs infrared radiation to such an extent that its total internal energy exceeds the dissociation limit corresponding to the least endothermic path. Even though the initial excitation energy in the ions here is provided by the ionization process rather than through multiple IR photon absorption, there

is a direct correspondence between the single absorption and subsequent dissociation. The present experiments are thus a sensitive probe of the final step in (low power) MPD of polyatomic molecular ions. In the high power MPD work, the photon flux and dissociation rate allow the energized molecule to continue absorbing photons beyond the dissociation threshold. In the present case, however, this is not possible as the up-pumping rate is too small compared with the unimolecular decomposition rate. This situation is reflected in the much smaller recoil energy distribution found here relative to the MPD studies. If the QC concept is valid, the dissociating ions studied here must certainly fall within that region, nonetheless, the process observed here corresponds to absorption by a specific vibrational mode as shown by the characteristic photodissociation yield with wavelength. It thus appears that, despite the high degree of excitation and the large density of states present, the oscillator strength tends to peak around the frequency of the fundamental molecular vibrational modes as has been postulated by Bloembergen and Yablonovitch.[1] Although the absorption process is mode specific, the dissociation channel is not, so that only the lowest energy pathway is observed as in MPD. Indirect evidence of this type of resonant absorption has recently been deduced from the power dependence of CH_3OHF^- MPD by Rosenberg *et al.*[19]

Using the high resolution (~ 1 MHz) Doppler-tuning capability previously described, the photodissociation of CF_3I^+ was further investigated. The CF_3^+ photofragment yield was measured over the full 250 MHz tuning range centered about several of the strongly absorbed laser lines. In each case, the yield was found to be essentially constant; that is, at 1 MHz resolution, the absorption process was continuous. Because of the large range of initial energy content in the absorbing ions, it is not unexpected that the overlapping spectra of these many excited species might lead to continuous absorption. Additional broadening can arise from variations in the vibrational anharmonicities of the highly excited ions. Such broadening might also account for the 30-cm^{-1} wide envelope measured for CF_3I^+ as compared with the 20-cm^{-1} width for the summed P, Q, and R branches for the neutral gas.

ACKNOWLEDGMENTS

The authors thank H. Helm and R. C. Dunbar for their enthusiastic participation in some of this work and E. Yablonovitch for a particularly stimulating discussion. Useful discussions were also held with D. L. Huestis, J. R. Barker, M. Rossi, J. I. Brauman, and R. N. Zare. This work was supported by the Office of Naval Research under Contract N00014-76-C-1035.

[1] N. Bloembergen and E. Yablonovitch, in *Laser-Induced Processes in Molecules*, edited by K. L. Kompa and S. D. Smith (Springer, Berlin, 1979), p. 117; N. Bloembergen and E. Yablonovitch, Physics Today 31(5), 23 (1978).
[2] P. A. Schulz, Aa. S. Sudbø, D. J. Kranovich, H. S. Kwok, Y. R. Shen, and Y. T. Lee, Ann. Rev. Phys. Chem. 30, 379 (1979).
[3] W. Forst, *Theory of Unimolecular Reactions* (Academic, New York, 1973); P. J. Robinson and K. A. Holbrook, *Unimolecular Reactions* (Wiley, London, 1972).
[4] B. A. Huber, T. M. Miller, P. C. Cosby, H. D. Zeman, R. L. Leon, J. T. Moseley, and J. R. Peterson, Rev. Sci. Instrum. 48, 1306 (1977).
[5] R. L. Woodin, D. S. Bomse, and J. L. Beauchamp, in *Chemical and Biological Applications of Lasers*, edited by C. B. Moore (Academic, New York, 1979), p. 355.
[6] R. N. Rosenfeld, J. M. Jasinski, and J. I. Brauman, J. Am. Chem. Soc. 101, 3999 (1979).
[7] A. Von Hellfeld, D. Feldmann, K. H. Welge, and A. P. Fournier, Opt. Commun. 30, 193 (1979).
[8] See, for example, J. T. Moseley, R. P. Saxon, B. A. Huber, P. C. Cosby, R. Abouaf, and M. Tadjeddine, J. Chem. Phys. 67, 1659 (1977); M. Tadjeddine, R. Abouaf, P. C. Cosby, B. A. Huber, and J. T. Mosley, J. Chem. Phys. 69, 710 (1978).
[9] R. E. Marcotte and T. O. Tiernan, J. Chem. Phys. 54, 3385 (1971).
[10] C. J. Noutary, J. Res. Natl. Bur. Stand. A 72, 479 (1968).
[11] These values were obtained from the compilation of H. M. Rosenstock, K. Draxl, B. W. Steiner, and J. T. Herron, J. Phys. Chem. Ref. Data 6, Suppl. 1 (1977). Systematic measurements have not been reported for all three halides. Thus the accuracies of the endoergicities within a given product channel are largely uncertain; however, the ordering of the energies among the channels is more certain.
[12] Aa. S. Sudbø, P. A. Schulz, E. R. Grant, Y. R. Shen, and Y. T. Lee, J. Chem. Phys. 70, 912 (1979).
[13] I. Oref and B. S. Rabinovitch, Acc. Chem. Res. 12, 166 (1979).
[14] P. R. McGee, F. F. Cleveland, A. G. Meister, C. E. Decker, and S. I. Miller, J. Chem. Phys. 21, 242 (1953).
[15] L. H. Sutcliffe and A. D. Walsh, Trans. Faraday Soc. 57, 873 (1961).
[16] E. K. Plyler and N. Acquista, J. Res. Natl. Bur. Stand. 48, 92 (1952).
[17] H. Jones and F. Kohler, J. Mol. Spectrosc. 58, 125 (1975).
[18] M. J. Coggiola, P. C. Cosby, H. Helm, R. C. Dunbar, and J. R. Peterson (to be published).
[19] R. N. Rosenberg, J. M. Jasinski, and J. I. Brauman (submitted to Chem. Phys. Lett.).

APPENDIX B

Photodissociation of molecular ions by absorption of single IR photons in the quasi-continuum

M. J. Coggiola, P. C. Cosby and J. R. Peterson
Molecular Physics Laboratory, SRI International
Menlo Park, California 94025 USA

Photodissociation of vibrationally excited CF_3I^+ and CF_3Br^+ ions by a cw CO_2 laser was observed under conditions in which only single photoabsorption could occur. The data thus yield information on the nature of absorptions in the vibrational quasi-continuum, and characterize the final step in multiphoton dissociation in the low power limit. Strong resonances are observed in both cases, and are ascribed to the C-F stretch mode.

Stimulated by the possibility of developing inexpensive methods for isotope separation and selectively inducing chemical reactions, considerable experimental and theoretical efforts have been directed, in the last five years, to understanding the processes of IR multiphoton dissociation (MPD) of molecules. Recently, the experimental emphasis has been directed to studies under collision-free conditions in order to simplify the interpretation of the results. The results of this research, which has been reviewed by Bloembergen and Yablonovitch[1] and by Schulz et al.,[2] have led to the development of a qualitative model which lacks much detail but nevertheless gives a reasonable description for the behavior of many molecules under pulsed laser excitation. The model may be summarized as follows: The first several quanta are absorbed stepwise in resonance with one of the major absorbing vibrational-rotation transitions. Red shifts due to anharmonicities following the first absorption are accomodated by power broadening. However, after these few quanta have been absorbed in a single mode, the existence of other (N-1) normal modes in the molecule makes it possible for energy contained in the initially excited mode to become rapidly distributed among them. It is now commonly accepted that in polyatomic molecules, this redistribution begins to occur when the density of states of all other modes corresponding to that total energy content in the molecule, becomes sufficiently high to form a "quasi-continuum" (QC) of energy levels. Suppose this occurs after n_1 photons have been absorbed. Subsequent absorptions occur at rates and with wavelength dependencies that characterize the absorption of the n_1th photon. After enough stepwise absorptions in the QC that the total energy contained in all modes exceeds the dissociation energy, the molecule can undergo unimolecular decomposition via the lowest energy channel.

This step can be described by RRKM theory.[3] One of the open questions raised by this model concerns the exact nature (i.e., absorption strength and wavelength dependence) of these absorptions in the QC. From the nature of some MPD experiments and from theoretical arguments it appears that the absorption profile in the QC is considerably broader than for the first few resonant levels, and in fact is non-zero at wavelengths far away from the original resonance. However, it has also been suggested[1] that some resonant characteristics may still exist in the QC.

Our experiment was originally aimed to make use of the very high (sub-Doppler) resolution obtainable in our coaxial laser-ion beam apparatus[4] to determine the details of the first few ir absorptions in molecules. However, due to one of the quirks of Mother Nature, these studies were precluded by a vibrationally hot beam, and we have instead been able to make some unique studies of photoabsorptions in the quasi-continuum. We find that strong resonance characteristics can exist even high in the QC near the dissociation limit.

The Experiment

The experiment was carried out on our laser-ion beam photofragment spectrometer, shown schematically in Fig. 1, with a CW CO_2 laser beam interacting coaxially with the mass-analyzed ion beam over a distance of about 33 cm. Either the parent beam ions or any photofragment ions formed in the interaction region may be subsequently electrically deflected into a drift space 1 m in length, and into the entrance aperture of a 180° electrostatic energy analyzer. We had previously found that the molecular ions are generally quite highly excited in our beams (the ions are produced by an electron beam of variable energy, normally 100 eV, but secondary electrons from surfaces undoubtedly broaden the energy spectrum). This excitation prevented successful studies of exciting lower vibrational levels but we found that it permitted photodissociation by the absorption of single photons. We had chosen to study fluorinated hydrocarbon ions, whose neutral parents are known to be strong absorbers of CO_2 laser photons in the C-F stretch mode. It was believed that C-F stretch frequencies in the ion would be fairly close to those of the neutrals and thus be in the frequency range of our CO_2 laser.

We first studied CF_3I^+ and CF_3Br^+. We found that both molecules were dissociated to CF_3^+ (the lowest energy channel) with a probability that was linearly dependent on the laser power (typically 1-3 Watts in the interaction region). There was also a competitive current of CF_3^+ caused by collisions with the background gas in the chamber (pressures $\sim 10^{-8}$ torr). This collisionally-induced dissociation signal was eliminated by chopping the laser beam. Figure 2 shows the laser frequency dependence for the CF_3I^+ photodissociation (PD). The PD probability exhibits a strong resonance peaked at about 947 cm^{-1} with a width of $\sim$ 30 cm^{-1} FWHM. The dependence of the peak probability on laser power is shown in Fig. 3. Because of the short residence time (6-8 μsec) of the ions in the interaction region and the low laser photon flux ($1\text{-}5 \times 10^{21}$ cm^{-2} sec^{-1}) there is a negligible probability for the absorption of more than one photon, in agreement with the linear

power dependence. We therefore conclude that a small fraction of the beam ions are internally excited to within $h\nu$ (0.12 eV) of the dissociation limit. The dissociation limit is about 1.3 eV for CF_3I^+ and 0.5 eV for CF_3Br^+. These photodissociations thus occur because of the absorption of a single photon in the QC, and the wavelength dependence is therefore characteristic of such absorptions. This experiment is the first direct observation of absorptions in the QC.

In the neutral CF_3I molecule, the mode closest to 947 cm^{-1} is the C-F stretch ν_1 mode at about 1073 cm^{-1}, thus an assignment of ν_1 to the resonance in CF_3I^+ would imply a 10% weakening of the C-F band in the ion. Strong support for this assignment is found in a far uv absorption study of CF_3I, where the vibrational spacings in at least one member of a Rydberg series leading to the ion were measured, and the ν_1 mode in the $7s\sigma$ state was found at $\sim$ 950 cm^{-1}.

We note in Fig. 2 that toward higher frequencies the cross section drops to 1% of the peak value, and then shows evidence of a second peak above 1075 cm^{-1}.

The PD spectrum for CF_3Br^+ demonstrated a similar strong peak at $\sim$ 953 cm^{-1} (FWHM $\sim$ 30 cm^{-1}). It also dropped to $\sim$ 1% of the peak value at higher frequencies but did not show a second increase in the observed frequency range ($\nu \leq 1090$ cm^{-1}). See Fig. 4.

We conclude that photoabsorptions in the vibrational quasi-continuum of CF_3I^+ and CF_3Br^+ show strong resonances characteristic of frequencies close to the ν_1 mode of the ground state. Furthermore, the widths are not much larger (5-10 cm^{-1}) than the envelope of the summed P, Q, and R branches of the ground state. We therefore conclude that the peak absorption cross section is not much smaller than that of the ν_1 ground state absorption.

This research was supported by the Office of Naval Research.

1. N. Bloembergen and E. Yablonovitch, in: Laser-Induced Processes in Molecules, K. L. Kompa and S. D. Smith, Eds. (Springen, Berlin, 1979) p. 117; N. Bloembergen and E. Yablonovitch, Physics Today 31(5), 23 (1978).

2. P. A. Schulz, Aa. S. Sudbø, D. J. Krajnovich, H. S. Kwok, Y. R. Shen, and Y. T. Lee, Ann. Rev. Phys. Chem. 30, 379 (1979).

3. W. Forst, "Theory of Unimolecular Reactions," Academic Press, N.Y. (1973), or P. J. Robinson, and K. A. Holbrook, "Unimolecular Reactions," Wiley, London (1972).

4. B. A. Huber, T. M. Miller, P. C. Cosby, H. D. Zeman, R. L. Leon, J. T. Moseley, and J. R. Peterson, Rev. Sci. Instrum., 48, 1306 (1977).

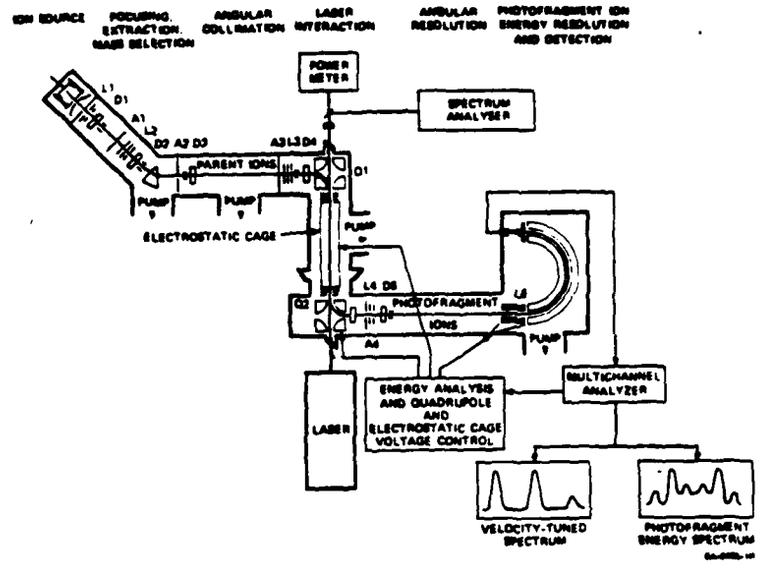

FIGURE 1 DIAGRAM OF THE APPARATUS

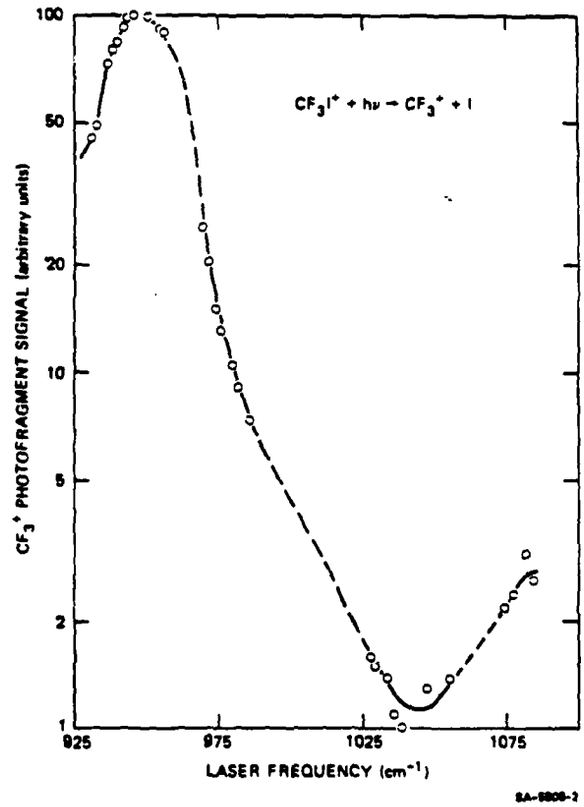

FIGURE 2 FREQUENCY DEPENDENCE OF THE CF_3^+ FRAGMENT YIELD FROM CF_3I^+ CORRECTED FOR LASER POWER VARIATIONS

Dashed line indicates CO_2 laser tuning gaps.

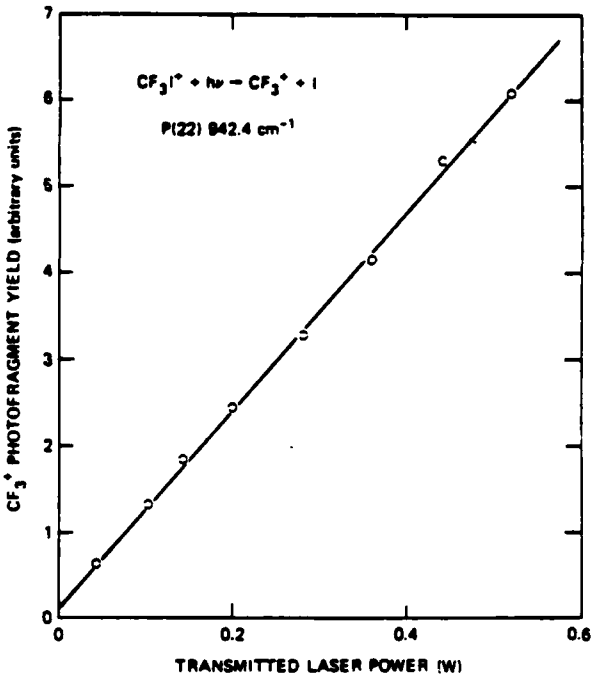

FIGURE 3

POWER DEPENDENCE OF CF_3I^* PHOTODISSOCIATION AT 942.4 cm^{-1}, P(22)

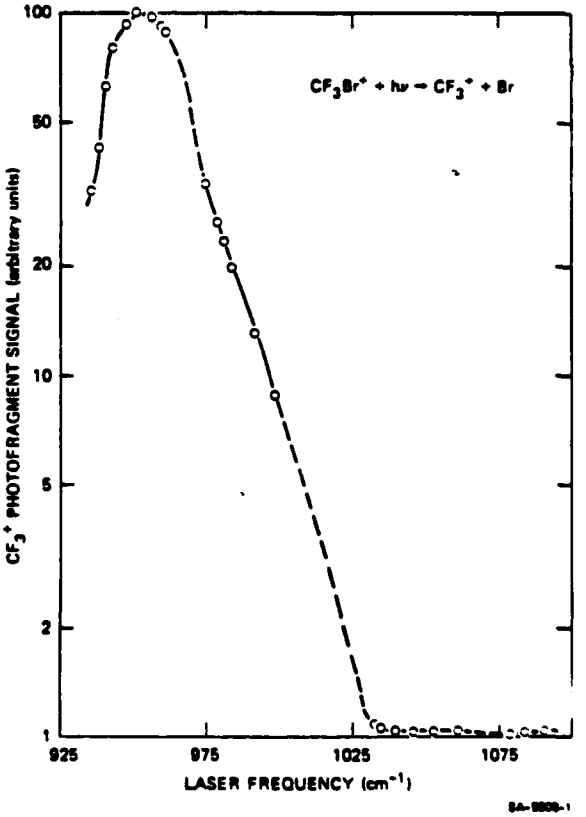

FIGURE 4

FREQUENCY DEPENDENCE OF THE CF_3^+ FRAGMENT YIELD FROM CF_3Br^* CORRECTED FOR LASER POWER VARIATIONS

APPENDIX C

PHYSICAL REVIEW A VOLUME 23, NUMBER 1 JANUARY 1981

Photodetachment cross sections for He^- ^4P

R. V. Hodges, M. J. Coggiola, and J. R. Peterson
Molecular Physics Laboratory, SRI International, Menlo Park, California 94025
(Received 17 June 1980)

Absolute photodetachment cross sections for He^- $^4P^o$ have been obtained at discrete photon energies between 0.12 and 4.0 eV by normalizing the He photodetachment products from a 1.3-keV He^- beam to those from autodetachment over a known path length, and making use of the known metastable lifetimes. The cross section reaches 1.2×10^{-16} cm^2 at 0.12 eV (40 meV above threshold), falls to 1×10^{-17} cm^2 at 4.0 eV, and exhibits several distinct features associated with excited He product states.

I. INTRODUCTION

The $1s2s2p$ $^4P^o$ state of He^- is an unusual member of the class of core-excited atomic states that lie in the electronic continuum but are metastable against both autoejection of electrons and radiative decay. In 1955 Holøien and Midtdal[1] showed theoretically that He^- ^4P lies energetically below its parent $1s2s$ ^3S state, and as it is metastable against autodetachment to the $^1S_0$ ground state, this result explained the experimental observation of He^- by Hiby in 1932.[2] Holøien and Geltman[3] later calculated the binding energy to be $\gtrsim$33 meV with respect to 2^3S. It was subsequently found to be 80 ± 2 meV by Brehm, Gusinow, and Hall[4] who measured the kinetic energies of photodetached electrons. Later the fine structure states of He^- were studied by Novick and co-workers, who measured their autodetachment lifetimes[5] and energy intervals.[6]

This ion offers an opportunity to study characteristics of doubly-excited atoms and to test theoretical calculations of energy levels and widths of higher autodetaching states. Numerous detailed calculations have been made of the He^- doublet resonances that appear in e-He scattering. However, comparatively little work has been done on the quartet states, many of which can likely be studied in very high resolution via photodetachment. Because of its low threshold energy for detachment, He^- also allows a study of the behavior of the photodetachment cross section over a wide range of photon wavelengths using available laser sources.

While determining the He^- electron binding energy, Brehm *et al.*[4] were also able to estimate (to within a factor of 2) the photodetachment cross section at 514.5 nm. However, until now no other photodetachment measurements have been reported.[7] We report here measurements of the photodetachment cross section of He^- at a number of discrete photon energies between 0.12 and 4.0 eV.[8]

II. EXPERIMENTAL METHOD

A 1300-eV beam of He^- was prepared from He^+ by two successive electron capture reactions in alkali vapor, as was first done by Donnally and Thoeming[9] using cesium, and later by Brehm *et al.*[4] and Novick *et al.*[5,6] using potassium. In this work, sodium was chosen as a target vapor because it has been shown[10] that the $He^+ + Na$ reaction yields 90% He 2^3S at our beam energies, whereas the other alkalies produce at least 30% 2^1S. The latter can yield only the doublet states of He^-, which rapidly autodetach.

We used an existing apparatus[11] which normally produces neutral rare-gas metastable atoms by single electron capture of the corresponding ion in an alkali vapor. The He^+ ion beam is formed by direct extraction from a dc discharge source. The beam is accelerated to its final kinetic energy and magnetically mass analyzed before being focused into a 6.7 cm long differentially pumped charge-exchange cell. Alkali vapor pressures of about 0.5 mtorr are used to produce neutral beams under single-collision conditions. However, in this experiment the Na vapor pressure was increased to ~10 mtorr where He^- production was about 0.1% of the incident He^+. In a separate vacuum chamber, the He^- component was electrostatically separated from He^0 and He^+ as shown in Fig. 1, and was intersected by a laser beam midway along a field-free drift region. Downstream, a second deflector removed residual ions leaving only neutral atoms formed from He^- in the drift region by photodetachment, autodetachment, or collisional detachment. These atoms entered the detector, where they struck a stainless steel surface at 45°, ejecting secondary electrons which were accelerated into a channeltron multiplier. Potentials on an entrance grid, the secondary emission surface, and the channeltron cone were adjusted to give optimum collection of the secondary electrons while rejecting electrons that originated outside the detector. The multi-

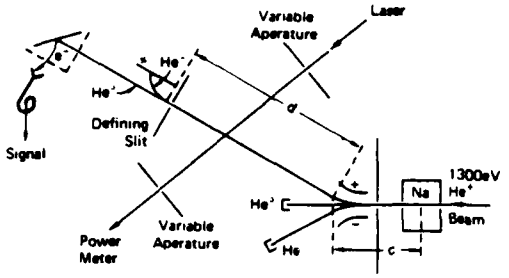

FIG. 1. Schematic diagram of the interaction region.

plier output was fed to appropriate pulse counting electronics. Several lasers were used as photon sources: a line-tunable cw CO_2 laser, cw Nd:YAG, argon and krypton ion lasers, and a pulsed rare-gas–halide excimer laser which was used alone and as a pump for a dye laser.

The photodetachment of a uniform ion beam of cross sectional area A, propagating along the x axis, and intersected by a laser beam propagating along the y axis, can be described by the equation

$$i_b/i_- = \sigma \int\int\int \frac{\Phi(x,z)}{A}\,dt\,dy\,dz, \quad i_b/i_- \ll 1 \qquad (1)$$

where σ is the photodetachment cross section, i_b is the equivalent current of photodetached He, i_- is the incident He^- current, and the integration extends over the time of interaction and the spatial overlap of the two beams in the y-z plane.

A major problem in obtaining reliable data was the evaluation of this integral. We found that consistent results could only be obtained by careful measurements of the laser-beam spatial distribution $\Phi(x,z)$, for each cross-section measurement. The laser beam was assumed to be cylindrically symmetric and thus $\Phi(x,z)$ could be expressed as $\Phi(r)$. This distribution was determined by measuring the laser power transmitted through each of two apertures of variable radius r at the entrance and exit windows of the interaction chamber. Measurements were made at six to eight values of r for each aperture by stopping down one aperture with the other fully open. The data were satisfactorily fitted to the Gaussian form

$$\Phi(r,\alpha) = P(\pi\alpha^2 h\nu)^{-1}\exp(-r^2/\alpha^2),$$

where P is the laser power, $h\nu$ is the photon energy, and α is the beam radius parameter. As the laser beam traversed the 1 m between apertures, α increased by 10–25%. The value of α at the laser-ion beam intersection was calculated assuming a linear change in α with distance. Values of α varied widely with laser power and wavelength, but the cross sections derived according to the procedure described below were internally consistent from day to day.

The height of the ion beam was defined by a 1.5-mm slit at the entrance to the final deflector. This slit was wide enough (8 mm) to accept the full width of the ~3-mm diameter ion beam parallel to the laser axis. For an ion beam of velocity v and height $2b$, Eq. (1) becomes

$$i_b/i_- = \sigma\int_{-b}^{b}\frac{1}{2b}\left[\int_{-\infty}^{\infty}\frac{P}{\pi\alpha^2 h\nu}\exp(-r^2/\alpha^2)\right]\frac{dx}{v}\,dz, \qquad (2)$$

$$= \frac{\sigma P}{vh\nu}\,\frac{1}{2b}\,\mathrm{erf}\left(\frac{b}{\alpha}\right). \qquad (3)$$

A noteworthy aspect of these experiments was the use of the metastability of He^- and the known lifetimes of the $J=\frac{1}{2}$, $\frac{3}{2}$, and $\frac{5}{2}$ substates to obtain absolute cross sections without determining the detector sensitivity. This was accomplished by normalizing the signal produced by photodetached neutrals to the steady background signal resulting from autodetachment ($\gtrsim 70\%$) and collisional detachment ($\lesssim 30\%$). The background signal i_b is described by

$$i_b/i_- = (R_a + k_c p)t = (R_a + k_c p)d/v, \quad i_b/i_- \ll 1 \qquad (4a)$$

where R_a and $k_c p$ are the autodetachment and collisional detachment rates, p is the pressure, and d is the distance between the two deflectors that define the ion drift path (see Fig. 1). The collisional detachment rate constant k_c was determined relative to R_a from the slope m of a plot of background signal versus pressure.[12] The pressure was altered by throttling the gate valve on the interaction chamber diffusion pump. Thus,

$$i_b/i_- = R_a(1 + mp)d/v. \qquad (4b)$$

The three He^- sublevels, $^4P_{5/2}$, $^4P_{3/2}$, and $^4P_{1/2}$, autodetach with lifetimes of 500 ± 200, 10 ± 2, and 16 ± 4 μsec, respectively.[5] Because the total fine structure splittings are less than 8 GHz (3×10^{-5} eV),[6] and the polarizabilities of all three states are expected to be equal, the population of the $\frac{5}{2}$, $\frac{3}{2}$, and $\frac{1}{2}$ He^- ^4P states formed from the electron capture of He 2^3S in sodium should be purely statistical. Novick and Weinflash[5] found this to be the case for He^- produced in potassium, and there is no intrinsic difference in production via the sodium reaction. The autodetachment rate, R_a, in the drift region d was thus calculated from the expression

$$R_a = \frac{f_{5/2}}{\tau_{5/2}} + \frac{f_{3/2}}{\tau_{3/2}} + \frac{f_{1/2}}{\tau_{1/2}}, \qquad (5)$$

where f_n is the fraction of the population in the nth sublevel and τ_n is the corresponding lifetime.

The population fractions are approximately constant during the beam's passage through the short drift region, but differ slightly from the original statistical distribution by small factors easily calculable from the lifetimes and the 1.7-μsec flight time from the point of formation to the drift region (region c in Fig. 1). The length of region c was estimated by assuming that the majority of the He^- ions were formed near the center of the charge-transfer oven. This assumption leads to a value of $c = 43.6$ cm. The uncertainty introduced by this assumption is much smaller than that due to the uncertainties in the lifetimes. The second field-free drift region (region d in Fig. 1) extends between the points within the two deflectors at which tangents to the ion trajectory are just able to enter the detector. This distance was calculated from the deflector geometry and the detector aperture radius to be 5.1 cm. Evaluation of Eq. (5) using these values gives $R_e = (4.1 \pm 0.7) \times 10^4$ sec^{-1}.

Equations (3) and (4) are readily combined to yield an expression for σ as follows:

$$\sigma = \frac{i_s}{i_b} \frac{R_e(1+mp)d2bh\nu}{P\sin(60)\,\mathrm{erf}(b/\alpha)} . \tag{6}$$

The factor sin(60) corrects for the fact that our laser-ion beam intersection angle is 60° rather than 90°.

The ratio method used here assumed that all neutral He products are detected with equal efficiencies. While the autodetached neutrals are $^1S_0$, the photodetached products are detected as 2^3S. Since all product detection is via single particle counting, it is only necessary that these two species have secondary electron-ejection coefficients (γ) in excess of unity at 1300 eV for them to be detected with equal probability. Independent measurements[13] of the secondary ejection coefficients were made at 45° incidence for the ground state ($\gamma \approx 1.5$) and excited He atoms ($\gamma^* \approx 1.9$) verifying that this requirement was met.

The experiment was performed by chopping the photon beam and accumulating the counts from the neutral He detector corresponding to laser on and off in the two channels of a PAR model 1112 processor. The ratio i_s/i_b is given by the ratio of the difference count to the background count. This ratio varied between 10^{-4} and 10^{-2} depending on laser power and wavelength.

In the pulsed laser experiments at 308 and 380 nm, time-of-arrival spectra of neutral He following the laser pulse were obtained with a time-to-amplitude converter and a multichannel analyzer operated in the pulse-height analysis mode. Photodetached He atoms appeared as a peak superimposed on a continuous background of autodetached and collisionally detached He. The cross section was calculated by normalizing the area under the peak to the background using a formalism similar to that described for the cw case.

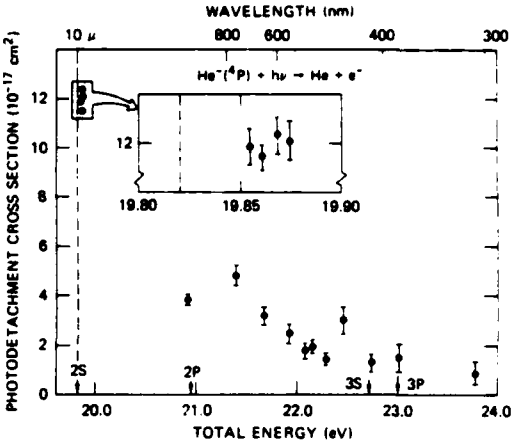

FIG. 2. Photodetachment cross section as a function of total energy relative to $He\,^1S_0$ (lower scale) and photon wavelength (upper scale). The arrows indicate outgoing excited He states.

III. RESULTS AND DISCUSSION

Results are presented in Fig. 2, and listed in Table I. The error bars shown are the relative uncertainties, which include the statistical counting uncertainty, and the relative uncertainties in α, P, and b. An absolute uncertainty of ±30% is assigned to the data on the basis of the uncertainties in the autodetachment rate (16%),[14] $k_c p$ (10%), d (10%), and the laser-ion beam overlap (15%).

The data in Fig. 2 are plotted against the total

TABLE I. Absolute $He^-2\,^4P$ photodetachment cross sections.

λ(nm)	Laser	$\sigma(10^{-17}$ cm$^2)$
10741	$CO_2 - P(34)$	11.8
10275	$CO_2 - R(16)$	11.4
9657	$CO_2 - P(32)$	12.3
9282	$CO_2 - R(18)$	12.0
1060	Nd:YAG	3.9
752.5	Kr*	4.7
647.1	Kr*	3.3
568.2	Kr*	2.5
530.9	Kr*	1.8
514.5	Ar*	2.0
488.0	Ar*	1.3
457.9	Ar*	3.0
413.1	Kr*	1.3
380.0	XeCl + BBQ	1.5
308.0	XeCl	0.8

electronic energy relative to He $^1S_0$, $E = h\nu + 19.74$ eV, assuming that He$^-$ ^4P lies 80 meV below He 2^3S, as measured by Brehm *et al.*,[4] although recent calculations argue for a slightly lower value.[15] The locations of the lowest He triplet states are indicated on the abscissa. The 2^3S photodetachment threshold is indicated by a vertical dashed line. At this threshold, the transition $1s2s2p + h\nu \rightarrow 1s2s\,2^3S + \epsilon s$ (or ϵd) yields predominantly s-wave electrons, and the cross section should behave[16,17] as $\nu(\nu - \nu_0)^{1/2}$, with an infinite slope at ν_0. The four CO_2 laser measurements near 10 μm are roughly equally spaced in energy between 35 and 53 meV above the threshold, as shown in the energy-magnified inset in Fig. 2. These points represent the largest cross sections observed. Considerably care was taken to reduce the uncertainties in these points. The lack of any strong energy dependence among them suggests that the maximum cross section is not much larger. It also indicates that the Wigner threshold law[16] does not extend this far above threshold because a $\nu(\nu - \nu_0)^{1/2}$ curve drawn from the 2^3S threshold through this region passes through the data in the expanded inset in Fig. 2 at about 70° to the horizontal and clearly does not fit the data. This result is not surprising; Hotop, Patterson, and Lineberger[18] found that the Wigner law is obeyed only within 5 meV of threshold for Se$^-$ $^2P_{3/2} + h\nu \rightarrow$ Se $^3P_2 + \epsilon s$.

Photodetachment cross sections (for a single outgoing state) generally peak at photon energies within a few times the threshold value and then fall off monotonically toward zero. If He$^-$ behaves similarly, the cross section should peak at a total energy of ≤20 eV, and then fall off toward higher energies, at least to the 2^3P threshold at 20.96 eV. The photodetachment cross section at 20.91 eV, measured with a cw Nd:YAG laser (1.06 μm), lies below this threshold, and is thus expected to follow the smooth falloff from the peak value near 20 eV. However, the envelope established by extrapolating the points between 22.8 and 21.4 eV toward the 20.96-eV 2^3P threshold, indicates that a substantial increase in the cross section (by perhaps a factor of 2) occurs as the photon energy is increased through the 2^3P threshold. This increase would be more gradual than at the 2^3S threshold because here it involves an outgoing p wave ($1s2s2p\,^4P - 1s2p\,^3P + \epsilon p$), and excluding interference effects the cross section should have a $\nu(\nu - \nu_0)^{3/2}$ threshold behavior.[17]

The point at 22.45 eV (from the 457.9-nm Ar^+ laser line) lies well above the envelope. We assume that this point is connected with a Feshbach resonance lying below the 3^3S state, possibly $1s3s^2d\,^4D^e$, which could rapidly autodetach and thus be fairly broad. Compton *et al.*[7] have also found a resonance in the vicinity of 470 nm. Oberoi and Nesbet[19] have calculated cross sections for electron scattering from He 2^3S and report a $^4D^e$ resonance at 22.56 eV with a width of 0.01 eV, which would correspond to a wavelength of 440 ± 1.5 nm.

The two highest energy points were measured using a pulsed XeCl excimer laser both directly at 308 nm, and to pump a dye (BBQ) at 380 nm. The latter wavelength corresponds approximately to the 3^3P threshold at 23.01 eV. The dye laser was used to search for resonance effects at a number of close-lying wavelengths between 377 and 382 nm. However, the dye laser output was unstable from pulse to pulse both in profile and position, and the resulting scatter in the data was too great to detect small structure. We have therefore averaged all these dye laser data to yield a single value at 380 nm. This point seems to lie above the envelope and could result from an increase above the 3^3P threshold, but the uncertainties are too large to attach much significance to it.

The only previously reported photodetachment cross section of He$^-$ is the estimate of $\sigma = 6 \times 10^{-18}$ cm^2 ($\pm 2x$) at 514.5 nm by Brehm *et al.*,[4] who measured electrons ejected in the direction of the electric vector of the laser photons. The present value of $(2.0 \pm 0.6) \times 10^{-17}$ cm^2 is larger, but possibly within the combined uncertainties. Because their experiment was primarily aimed at the measurement of electron energies rather than cross sections, we do not consider the disagreement to be serious.

When only one outgoing channel exists, such as below the 2^3P threshold, it is straightforward using detailed balancing[17] to calculate the radiative attachment cross sections $\sigma_a(E_e)$, where E_e is the electron energy for $e + \text{He}\,2^3S \rightarrow \text{He}^-\,^4P + h\nu$. We find at 10 μm, σ_a (0.04 eV) $= 1.6 \times 10^{-22}$ cm^2, and below the 2^3P threshold, σ_a (1.09 eV) $= 1.2 \times 10^{-22}$ cm^2. The corresponding radiative attachment rates are 1.4×10^{-15} cm^3 sec^{-1} and 1.1×10^{-14} cm^3 sec^{-1}, respectively. Because we do not know the final state branching ratios at higher photon energies, further calculations would be speculative. The inability to distinguish between different product channels is the main shortcoming of this experimental method. Its advantage for cross section measurements is the simplicity of collecting all products regardless of the photon wavelength or of the final state of the He atom.

IV. CONCLUSIONS

These measurements are clearly incomplete, in that no details of resonance characteristics were

studied, but they do show the general aspects of the cross-section magnitude and its dependence on photon energy. These absolute photodetachment cross sections provide a useful test for various approximate methods of calculating oscillator strengths of bound-free transitions for weakly bound electrons. The 1.2 $Å^2$ peak cross section measured here is nearly three times larger than that for H^- ($EA = 0.75$ eV) but is close to that calculated[20] for Li^- ($EA = 0.62$ eV). Further experimental studies in the region between the threshold (~15.5 μm) and the first maximum (~5–8 μm) would be very useful. Other important areas for further research are in the 300–500-nm region, which should include much resonance structure associated with the He^- quartet states analogous to the doublet states recently calculated by Nesbet,[21] and the 0.8–2 μm region which should include the $^4P^e$ resonance structure as well as the 2^3P threshold behavior.

This work was supported by the Office of Naval Research. We have benefited from conversations with D. L. Huestis and K. T. Gillen.

[1]E. Holøien and J. Midtdal, Proc. Phys. Soc. London Sec. A 68, 815 (1955).
[2]J. W. Hiby, Ann. Phys. Leipzig 34, 473 (1939).
[3]E. Holøien and S. Geltman, Phys. Rev. 153, 81 (1967).
[4]B. Brehm, M. A. Gusinow, and J. L. Hall, Phys. Rev. Lett. 19, 737 (1967).
[5]R. Novick and D. Weinflash, in *Precision Measurement and Fundamental Constants (Proceedings of the International Conference at Gaithersburg, Md., 1970)*, edited by D. N. Langenberg and B. N. Taylor, National Bureau of Standards Special Publication No. 343 (U. S. GPO, Washington, D. C., 1971), pp. 403–410.
[6]D. L. Mader and R. Novick, Phys. Rev. Lett. 29, 199 (1972); 32, 185 (1974).
[7]Measurements are also being carried out currently at Oak Ridge National Laboratory by R. N. Compton and co-workers, J. Phys. B (unpublished).
[8]For a preliminary report, see: R. V. Hodges, M. J. Coggiola, J. R. Peterson, Abstracts of the 7th International Conference on Atomic Physics, Massachusetts Institute of Technology, Cambridge, 1980 (unpublished), p. 180.
[9]B. L. Donnally and G. Thoeming, Phys. Rev. 159, 87 (1967).
[10]C. Reynaud, J. Pommier, Vu Ngoc Tuan, and M. Barat, Phys. Rev. Lett. 43, 579 (1979).
[11]M. Hollstein, D. C. Lorents, J. R. Peterson, and J. R. Sheridan, Can. J. Chem. 47, 1858 (1969).
[12]Systematic measurements of the absolute collisional detachment cross section of He have recently been completed, M. J. Coggiola and R. V. Hodges (unpublished).
[13]R. V. Hodges, M. J. Coggiola, and K. T. Gillen (unpublished results).
[14]This uncertainty value was calculated assuming that the uncertainties in the three lifetimes were independent.
[15]A. V. Bunge and C. F. Bunge, Phys. Rev. A 19, 452 (1979) have calculated a binding energy of 77.4 meV with a reported accuracy of 0.2 meV. This value would shift all energies in Fig. 2 downward by 2.6 meV.
[16]E. P. Wigner, Phys. Rev. 73, 1002 (1948).
[17]H. Massey, *Negative Ions* (Cambridge University Press, London, 1976), p. 418.
[18]H. Hotop, T. A. Patterson, and W. C. Lineberger, Phys. Rev. A 8, 762 (1973).
[19]R. S. Oberoi and R. K. Nesbet, Phys. Rev. A 8, 2969 (1973).
[20]D. L. Moores and D. W. Norcross, Phys. Rev. A 10, 1646 (1974).
[21]R. K. Nesbet, J. Phys. B 11, L21 (1978).

APPENDIX D

PHOTODETACHMENT AND COLLISIONAL DESTRUCTION OF He^-

Michael J. Coggiola

Molecular Physics Laboratory
SRI International
Menlo Park, California 94025

Measurements of the destruction cross sections of the metastable negative He^- ion are reviewed, including both photodetachment and collisional detachment. Recent results on the wavelength dependence of the photodetachment of He^- $(1s2s2p)\ ^4P$ are presented in detail. New collisional destruction cross section results for a number of target gases are also given which extend the impact energy range down to 500 eV. Slow positive ion current measurements indicate the relative importance of target ionization for Ar and O_2. The nature of this Penning-type interaction is discussed.

MP 81-54
03/20/81

1. INTRODUCTION

Since its initial tentative observation by Hiby in 1939[1], the He^- ion has continued to be of considerable interest both theoretically and experimentally. As early as 1936, the $(1s^2 2s)\ ^2S$ "ground state" He^- ion was calculated to be unstable,[2] and so presumably not observable experimentally. Stimulated by its subsequent discovery, Holøien and Midtdal[3] were able to show that the $(1s2s2p)\ ^4P$ core-excited configuration should in fact be bound by at least 0.075 eV relative to the $(1s2s)\ 2^3S$ neutral atom. Nominally, at least, this ^4P state should be metastable against both direct autoionization and radiative decay to a ground state atom plus a free electron. However, it was readily recognized[3] that the $^4P_{1/2}$ and $^4P_{3/2}$ J-levels would mix with the corresponding ^2P states due to a partial breakdown of the LS coupling. Since the doublet states are short lived, the admixture of ^4P and ^2P would be expected to greatly reduce the lifetime of both the $^4P_{1/2}$ and $^4P_{3/2}$ states. Because there is no corresponding J = 5/2 doublet state, the $^4P_{5/2}$ level cannot autoionize via the same mechanism; however, it is still possible for it to autodetach via a weak spin-spin interaction.

Somewhat earlier, it had been found[4] that the $(2s2p^2)\ ^4P$ state of He^- was bound relative to both the $(2s2p)\ ^3P$ and $(2p^2)\ ^3P$ states of the neutral atom, however, this configuration is subject to rapid radiative decay to the $(1s2s2p)\ ^4P$ level. In addition, the lowest doublet states are found[3] to be unbound in the case of $(1s2s2p)\ ^2P$ or autoionizing in the case of $(1s2s^2)\ ^2S$. Thus, the $(1s2s2p)\ ^4P$ state of He^- is expected to be the only metastable configuration having an appreciable (μsec) lifetime. This expectation has been borne out by numerous experiments over the past 12 years.

While the initial observation of He^- was made in the ion source of a mass spectrometer, the subsequent studies[5-15] of He^- formation all involved produc-

tion by electron capture reactions beginning either with He^+ or neutral He atoms. Table I summarizes a number of these studies and includes reported estimates of the charge-transfer cross sections. In several of these experiments, there is some ambiguity as to the exact composition of the projectile beam, especially in those cases where a neutral He atom beam was itself formed by charge-exchange. Despite these uncertainties, two broad classes of experiments can be identified; those which suggest that the final He^- state is the $(1s2s2p)\ ^4P$, and those which tend to support a doublet final state, possibly the $(1s2p^2)\ ^2P$. Independent of the final state question, several of the experiments included in Table I clearly demonstrated the importance of the He^* $(1s2s)\ 2^3S$ metastable atom as an intermediate in the formation of He^- $(1s2s2p)$ ^4P.[10,13,15]

Donnally and Thoeming[10] were the first to point out that the two-step formation process involving the 2^3S intermediate should be a very efficient production method:

$$He^+ + X \rightarrow He^*\ (1s2s)\ 2^3S + X^+ \qquad (1a)$$

$$He^*\ 2^3S + X \rightarrow He^-\ (1s2s2p)\ ^4P + X^+ \quad . \qquad (1b)$$

They correctly reasoned that using an alkali (X = Cs,K in their experiments) as the target in both steps would lead to high yields of the He^- product owing to the very large σ_{1*} found by Peterson and Lorents.[16] They verified this experimentally, observing a 1.2% conversion efficiency for $He^+ \rightarrow He^-$ at 3 keV in Cs.[10] Recent measurements of the final state distributions for reaction (1a) at energies between 100 eV and 1.5 keV by Barat and co-workers[17] have in fact shown that both Cs and K produce large (30-50%) 2^1S components.

On the other hand, the He^+ + Na reaction yields essentially 100% metastable 2^3S. Since the 2^1S can only lead to unstable doublet negative ions, whereas the 2^3S can lead to the metastable quartet He^-, it would appear that the production of $(1s2s2p)\ ^4P\ He^-$ at energies near 1 keV can be maximized by using a Na charge-transfer target.

The results of several of the early charge-transfer experiments suggested that a doublet He^- ion could also be produced and observed in single collisions of He^+ with ground state He[7] and H_2.[6,9] The work of Baragiola and Salvatelli[14] further supported the existance of an observable doublet He^-, formed in their case by:

$$He\ (^1S) + Mg\ (^1S) \rightarrow He^-\ (^2P) + Mg\ (^2S) \qquad (2)$$

at 40 keV, where the doublet state was presumed to be the $(1s2p^2)$. They estimated a lower bound on the radiative lifetime of the $(1s2p^2)\ ^2P$ state of 5×10^{-8} sec. Additional evidence for the production of a doublet state of He^- is found in the work of Dunn et al.[15] By producing neutral He beams containing known fractions of either 2^1S or 2^3S, they were able to study separately the reactions:

$$He\ (2^1S) + H_2 \rightarrow He^-\ (^2P) + H_2^+ \qquad (3)$$

and

$$He\ (2^3S) + H_2 \rightarrow He^-\ (^4P) + H_2^+ \quad . \qquad (4)$$

At 200 keV, they found

$$\sigma_{*-1}\ (2^1S) = 1.1 \times 10^{-18}\ cm^2$$

and

$$\sigma_{*-1}\ (2^3S) = 2.0 \times 10^{-18}\ cm^2 \quad .$$

The large $\sigma_{*-1}\ (2^1S)$ cross section clearly lends credence to their conclusion that a long-lived doublet state can in fact be produced by charge-transfer. Dunn et al. were also able to place a lower limit of 10^{-6} sec on the lifetime of this state.

Unfortunately, the recent theoretical study of Bunge and Bunge[18] could find no evidence for the existence of such long-lived doublet states.

2. PROPERTIES OF He^-

Beyond determining the configuration of the long-lived state(s) of He^-, considerable efforts have been directed at obtaining values of the electron binding energy and autodetachment lifetimes. Determinations of these two properties, and to a lesser extent the ^4P J- level energy separations, have provided inevitable and valuable comparisons between experiment and theory.

As noted in the introduction, Holøien and Midtdal[3] were the first to calculate a positive electron affinity for He^- $(1s2s2p)\ ^4P$ relative to He^* $(1s2s)\ 2^3S$. Their value of $EA \gtrsim 0.075$ eV appears to be in excellent agreement with more recent calculations (0.0774 eV)[18] and experiments (0.080 eV).[19] However, Holøien and Midtdal later discovered[20] an error in their original calculation which when corrected reduced the electron affinity to 0.0056 eV. An improved estimate of the EA was made by Holøien and Geltman[21] who obtained a lower bound of 0.033 eV. Somewhat later, Weiss[22]

reported a value of 0.067 eV, and more recently, Bunge and Bunge[18] find EA = 0.0774 ± 0.0003 eV. The accuracy of this latter result exceeds by nearly an order of magnitude the stated uncertainty in the only directly measured value of the electron binding energy in He^- by Brehm, Gusinow, and Hall, 0.080 ± 0.002 eV.[19]

Although perhaps not as accurate as the calculations of Bunge and Bunge, this experiment showed for the first time that He^- formed in charge-exchange of He^+ in K had the expected $(1s2s2p)\ ^4P$ configuration. By measuring the kinetic energy of electrons photodetached from He^- at a fixed wavelength, Brehm et al. were able to distinguish between photodetachment corresponding to loss of either the 2s or 2p electron. The reported 80 meV average value of the electron affinity was determined relative to the known EA of D^- which they observed simultaneously.

As a result of the different decay mechanisms, the three $^4P_{J=5/2,3/2,1/2}$ He^- states are expected to demonstrate "differential metastability," that is they should exhibit distinct lifetimes. Early attempts to calculate the lifetimes of the J = 5/2 level proved inconclusive[22-25] yielding values between 266 μsec and 1.7 msec. Experimentally, Nicholas et al.[26] measured the decay of a He^- beam over 1 and 2 meter flight paths to obtain a single component lifetime of 18.2 ± 2.7 μsec.

Using time-of-flight techniques to observe the differential decay of a He^- beam in an axial magnetic field, Blau, Novick, and Weinflash[27] and later Novick and Weinflash[28] were able to separate fast and slow decay components. The longer-lived component, associated with the J = 5/2 level was found to have a lifetime $\tau_{5/2}$ = 500 ± 200 μsec. The shorter-lived component of the He^- beam was resolved into two components to give $\tau_{3/2}$ = 10 ± 2 μsec and $\tau_{1/2}$ = 16 ± 4 μsec. These results have essentially been substantiated by

the work of Simpson et al.[29] More recently, Compton et al. have measured a short-lived component lifetime of 10.5 ± 2 μsec for He^- formed by He^+ charge-transfer in Ca vapor.[30] Improved theoretical calculations now give a reliable estimate of 455 μsec for the J = 5/2 lifetime.[31]

In addition to obtaining the lifetimes, both Novick and Weinflash[28] and Simpson et al.[29] found that the He^- decay curves were consistent with the J-levels being populated in proportion to their statistical weights. This result is reasonable in view of the very small energy level separations $\Delta_{53} = 3.41 \times 10^{-6}$ eV and $\Delta_{51} = 3.58 \times 10^{-5}$ eV found by Mader and Novick.[32] A similar statistical behavior is found in the charge-transfer of $Ne^+ + Na$.[33,34]

3. PHOTODETACHMENT OF He^-

The techniques of negative ion photodetachment are well established, and have been successfully applied to a large number of stable negative ions.[35] However, with the exception of the EA measurements of Brehm et al.,[19] photodetachment studies of the He^- ion have not been attempted until recently. One goal of such studies is the observation and identification of resonances in the detachment cross section as a function of photon energy. These resonances give information on excited electronic states. While there have been many numerical calculations of excited doublet state resonances which appear in e-He scattering, the corresponding quartet excited states have received little attention. Since the detachment threshold of He^- is small (0.077 eV) as is the threshold for ionization of the "parent" He^* $(1s2s)\ 2^3S$ (4.77 eV), a large number of excited electronic states might be expected to lie within an accessible wavelength range (16 μm - 260 nm).

The first reported studies of the photodetachment cross section of He^- were done in our laboratory at SRI[36] and at the Oak Ridge National Laboratory by Compton and co-workers.[37] A brief description of the former experiment will be given below, and results from both groups presented.

A. Experimental Method

The He^- beam was generated by charge-exchange of a mass selected He^+ beam in Na at 1300 eV, as shown in Figure 1. The Na vapor pressure was maintained at $\sim$ 10 mtorr where the He^- yield was about $\approx$ 0.1% of the incident He^+ current. The He^- was electrostatically separated from the $He^{+,o}$ components and intersected by a laser beam midway along a field-free drift region. Downstream from the detachment region, a second deflector removed any residual ions leaving only neutral atoms formed in the drift region. These neutral atoms, arising from photodetachment, collisional detachment, and autodetachment, entered the detector where they struck a stainless steel surface at 45° ejecting secondary electrons which were accelerated into a channeltron multiplier and counted. Bias potentials on the secondary emission surface, the channeltron cone, and an entrance grid were adjusted to maximize secondary electron collection while rejecting electrons that originated outside the detector. A number of lasers were used to obtain discrete photon energies in the range from 10 μm to 300 nm, including a line-tunable cw CO_2 laser, cw Nd:YAG, krypton and argon ion lasers, and a pulsed XeCl excimer laser which was used alone and as a pump for a dye laser.

In order to determine the absolute magnitude of the photodetachment cross section without requiring a knowledge of our overall detection sensitivity, we made use of the metastability of He^- and the measured lifetimes of the three substates. By normalizing the neutral photodetachment signal to the steady

background signal produced by autodetachment and collisional detachment over a known path length (region d, Figure 1), it is possible to determine the absolute photodetachment cross section.

One additional consideration needed to obtain accurate cross section values is the spatial overlap of the ion and photon beams. The photodetachment of a spatially uniform ion beam of cross sectional area A, propagating along the x axis, and intersected by a laser beam propagating along the y axis, can be described by the equation:[36]

$$i_p/i_- = \sigma \iiint \frac{\Phi(x,z)}{A}\, dtdydz \quad i_p/i_- \ll 1 \qquad (5)$$

where σ is the photodetachment cross section, i_p is the equivalent current of photodetached He, i_- is the incident He^- current, and the integration extends over the time of interaction and the spatial overlap of the two beams in the y-z plane. By carefully determining the spatial distribution of the laser beam, $\Phi(x,z)$ for each cross section measurement, it was possible to evaluate the integral in (5).

With the assumption that the He^- J = 5/2, 3/2/ 1/2 substates are statistically populated, and have lifetimes of 500, 10 and 16 μsec, respectively, we calculate the autodetachment rate in region d to be $4.1 \pm 0.7 \times 10^4$ sec^{-1}. This decay rate includes a correction for the fact that the beam composition changes slightly between the point of formation and the beginning of region d (i.e., during its passage through region c). The measured photodetachment signal can then be combined with this autodetachment rate and the measured collisional detachment cross sections (see section 4) to yield an absolute photodetachment cross section.

B. Results and Discussion

The measured cross section results are shown in Figure 2 and listed in Table II. The estimated absolute uncertainty of the data is ± 30%. The data in Figure 2 are plotted as a function of the total electronic energy relative to ground state He, with the lowest four triplet states of the neutral atom indicated. The vertical dashed line corresponds to the threshold for the process $1s2s2p + h\nu \rightarrow 1s2s\ 2^3S + \varepsilon s$ (or εd). This threshold is expected to yield mainly s-wave electrons, and have a $\nu(\nu - \nu_o)^{1/2}$ functional dependence. The four CO_2 laser measurements shown in the inset of Figure 2 are roughly equally spaced between 35 and 53 meV above this threshold. The dashed line in the inset corresponds to the expected $\nu(\nu - \nu_o)^{1/2}$ threshold behavior, which clearly does not fit the nearly constant cross section observed. Other photodetachment studies have, in fact, shown that this threshold law is obeyed only within a few meV of threshold.[38]

Several features in the photodetachment cross section suggest the presence of resonance structure. The point at 20.91 eV, measured at 1.06 μm using the Nd:YAG laser, lies just below the threshold for the opening of the first excited (relative to the 2^3S) neutral state: $(1s2p)\ 2^3P$. The next point, taken at a photon energy of 1.65 eV (21.4 eV total energy) lies above the 2^3P threshold (20.96 eV), and shows that a substantial increase in the cross section must occur in the vicinity of this threshold. Recent theoretical calculations of the photodetachment cross section for $He^-\ ^4P$ by Hazi and Reed[39] confirm the existence of a very large peak just above the 2^3P threshold due to a $(1s2p^2)\ ^4P^e$ shape resonance. Although Holøien and Geltman[21] originally calculated this $(1s2p^2)\ ^4P^e$ state to lie 0.20 eV below the parent $(1s2p)\ 2^3P$, the more recent work of Safronova and Senashenko,[40] Bunge and Bunge,[41] and Hazi and Reed[39] all place the $^4P^e$ state above the 2^3P by 1.22 - 1.73 eV.

The point at 22.45 eV (2.71 eV photon energy) also appears to lie above the smooth envelope. A $(1s3s3d)\ ^4D^e$ Feshbach resonance has been calculated by Oberoi and Nesbet[42] to occur in the $e\text{-}He(2^3S)$ scattering cross section at 22.56 eV. This resonance, having a calculated width of 0.01 eV, would appear $\approx$ 0.15 eV below the 3^3S threshold. Since the $^4D^e$ state is expected to rapidly autodetach, this feature could be fairly broad, and the point at 22.45 eV may be associated with excitation of this state.

The single cross section point just at the 3^3P threshold (23.0 eV) also appears to be higher than the overall envelope of the cross section, although the experimental uncertainties here were too large to ascribe much significance to this. It is interesting to note, however, that Hazi and Reed[39] do find evidence for a weak $(1s3p^2)\ ^4P$ Feshbach resonance $\sim$ 0.18 eV below the 3^3P threshold.

Also shown in Figure 2 are the recent results of Compton, Alton, and Pegg.[37] Their experimental method differed from the present study in that a pulsed, tunable dye laser was used throughout, and the detached electrons were collected rather than the neutral products. To obtain absolute cross sections, they made use of the known O^- photodetachment cross section for calibration purposes. By measuring the kinetic energy of the autodetached electrons, Compton et al. were also able to show that the He^- formed from He^+ charge-transfer in Ca was indeed in the $(1s2s2p)\ ^4P$ state.

It is apparent from Figure 2 that over the range in photon energies where these two experiments overlap, reasonable agreement is found both in the overall shape of the cross section and the absolute value. Compton et al. also find some evidence of structure in the cross section near 22.3 eV, which they also note may be associated with the $(1s3s3d)\ ^4D^e$ resonance calculated by Oberoi and Nesbet.

Below the 2^3P threshold, there is only a single final state accessible, and hence the energy of the outgoing electron is known. In that case, it is possible using detailed balancing to calculate the radiative attachment cross section, $\sigma_a(E_e)$, where E_e is the electron energy for $e + He(2^3S) \rightarrow He^-(^4P) + h\nu$. At the longest wavelength, 10 μm, $\sigma_a(0.04\ eV) = 1.6 \times 10^{-22}\ cm^2$ and at 1.06 μm, $\sigma_a\ (1.09\ eV) = 1.2 \times 10^{-22}\ cm^2$. At shorter wavelengths, the final state distributions are not known, and so the radiative attachment cross sections cannot be determined in this way.

4. COLLISIONAL DESTRUCTION OF He^-

Cross sections for the collisional destruction of He^- in He, Ar, H_2, and N_2 have been measured by a number of groups.[43] These studies have covered an energy range between 3 MeV and 4 keV. As expected for a loosely bound system such as He^-, the collisional detachment cross sections observed are large at all energies, typically showing a decrease with increasing collision energy. For example, Heinemein et al.[44] measured $\sigma_{-10} = 1.3 \times 10^{-16}\ cm^2$ for H_2 at 3 MeV, while Simpson and Gilbody[45] find $\sigma_{-10} = 19 \times 10^{-16}\ cm^2$ at 10 keV. For different target gases, the cross sections generally decrease in the order: $N_2 \approx Ar > Ne > H_2 > He$.

Using the attenuation techniques pioneered by Gilbody and co-workers,[46] Pedersen and Hvelplund[47] measured the apparent fraction of metastable neutral He formed by collisonal detachment of He^- in H_2 at 50 keV. Their finding that only 61% of the detached atoms were produced in the metastable state was somewhat surprising, assuming that the incident He^- was in the $(1s2s2p)\ ^4P$ state. Provided that no spin flip occurs, the detachment process is expected to be:

$$He^- (1s2s2p)\ ^4P + M \longrightarrow He\ (1s2s)\ 2^3S + M + e \qquad (6)$$
$$\longrightarrow He\ (1s2p)\ 2^3P + M + e$$
$$\xrightarrow{h\nu} He\ (1s2s)\ 2^3S$$

They advanced two possible explanations for the origin of the large fraction of ground state product observed: (1) The incident He^- actually contained a significant amount of a long-lived doublet, and hence the process:

$$He^- (1s2p^2)\ ^2P + M \rightarrow He\ (1s2p)\ 2^1P + M + e \qquad (7)$$
$$\xrightarrow{h\nu} He\ (1s^2)\ ^1S$$

becomes allowed; or (2) A Penning-type process occurs in which the weakly screened He^+ core captures an electron into the 1s orbital and subsequently ejects the two outer electrons,

$$He^- (1s2s2p)\ ^4P + M \rightarrow He^- (1s^2 2s) + M^+ + e \rightarrow He\ (1s^2) + M^+ + 2e$$

or (8)

$$He^- (1s2s2p)\ ^4P + M \rightarrow He^- (1s^2 2p) + M^+ + e \rightarrow He\ (1s^2) + M^+ + 2e$$

The same result will occur even if the ordering of the two steps is reversed, that is if the He^- is first collisionally detached to yield a metastable atom which then Penning ionizes the target before the two particles separate,

$$He^- \, (1s2s2p) \; ^4P + M \rightarrow He^* \, (1s2s) \; 2\,^3S + M + e \qquad (9)$$
$$\quad \longrightarrow He \, (1s^2) + M^+ + e$$

This type of mechanism has been previously suggested as being important in the quenching of excited atoms.[48-50] Processes (8) and (9) would not only lead to the production of ground state projectile atoms, but also to the production of slow positive target ions. Furthermore, since (8) and (9) involve a Penning-type interaction, they would not be expected to contribute to the detachment cross section in those cases where the Penning channel is closed, such as for He and Ne targets.

Pedersen et al.[51] later extended the energy range of these metastable fraction measurements for He^- detachment in He, Ne, Ar, H_2, and N_2 to between 25 and 400 keV. They again found that in general, between 30 and 60% of the collisonally detached He atoms are in the ground state. They were able to account for these results using a simple model which assumed that the short-lived (10 - 16μsec) component of the He^- beam was actually due to $(1s2p^2)$ ^2P, while the long-lived component was the quartet state. Later work by Pedersen,[52] however, showed that due to a possible systematic error in the earlier studies, the actual ground state fraction may have been considerably smaller than the reported value.

Electron detachment cross sections for He^- ^4P in various gases have been calculated using the classical impulse approximation of Bates and Walker.[53,54] This model calculates the classical energy transfer between the loosely bound electron and the target. If the amount of energy transferred exceeds the EA of the ion, then detachment is assumed to occur with unit probability. For the weakly bound He^- ion, this approximation is expected to be very reasonable, at least at higher energies.

In actual practice, Heinemein et al. calculated classical detachment cross sections for Ar, H_2, and He targets, and found excellent agreement with their data at energies down to 100 keV.[44] Conversely, the calculated cross sections of Snyder[55] are in reasonable accord for H_2, 20% low for He, and a factor of ~ 2 low for Ar at energies down to 4 keV.

We have recently completed measurements of the total collisonal destruction cross sections of He^- in He, Ne, Ar, H_2, O_2, and NO at energies from 4 keV to 500 eV.[56] In addition to these attenuation measurements, we have also made preliminary measurements of the slow positive ion current due to target ionization in an attempt to assess the relative importance of processes (8) and (9).

A. Experimental Method

The same scattering apparatus was used for this work as for the photodetachment studies with only a few modifications. As shown in Figure 3, a 1.5 cm long gas cell was introduced into the He^- beam path. The cell had a 1.5 mm entrance aperture and a 4 mm exit aperture. The current of He^- was monitored after the cell with a suppressed Faraday cup. A pair of condensor plates between the target cell and the Faraday cup could be used to either sweep away all charged species or to separate the $He^{+,o,-}$ components. In the latter case, the Faraday cup could be repositioned such that the current of any single species could be measured independently of the others. Not shown in Figure 3 is a small collector plate inside the collision chamber which could be biased to measure either slow positive or negative currents.

The effective length of the cell was determined by remeasuring the well-known $He^+ + He$ charge-exchange cross section[57,58] using an attenuation method. The length thus determined was $\sim 25\%$ greater than the geometric length.

B. Results and Discussion

The attenuation of the He^- current measured at the detector is related to the gas density in the cell, n, and the effective length, l, by the equation,

$$\ln(i/i_0) = (\sigma_s + \sigma_{-10} + 2\sigma_{-11})nl \qquad (10)$$

where i is the attenuated current, i_0 is the incident current, σ_s is the cross section for elastic scattering outside the detector viewing range, σ_{-10} is the total cross section for all processes which yield neutral products, and σ_{-11} is the cross section for the two electron loss. Since the detector viewing angle is ± 4°, it seems unlikely that σ_s will contribute to the observed attenuation, even at the lowest energies, hence this term in neglected. Several measurements of σ_{-11} have been made for He at the higher collision energies[44,47,59] and the results always show that $\sigma_{-11} \ll \sigma_{-10} + \sigma_{-1*}$. As a further check of this, we positioned the Faraday cup to collect only He^+ formed by two electron detachment. For He, Ar, and O_2 targets at 1 and 2 keV, we found no significant current of He^+ produced and as such we can set an upper limit of $\sigma_{-11} < 0.05\ \sigma_{-10}$. Values of σ_{-10} are thus assumed to equal the total attenuation cross section determined from the slope of semilog plots of current vs. gas density.

Results for σ_{-10} for the rare gases He, Ne, and Ar are presented in Figure 4. The corresonding total detachment cross sections for the diatomic targets are given in Figure 5. In both figures, the solid points at 4 keV represent the σ_{-10} cross sections measured by Simpson and Gilbody.[45] Agreement between the two sets of measurements is reasonable, although no explanation is apparent to account for the systematically higher cross sections measured in the present work.

The current of slow positive ions ($i_{slow\ +}$) and negative ions and electrons ($i_{slow\ -}$) produced in the attenuation cell were collected for He, Ar, and O_2 targets at several collision energies. Several tests were made to access the overall collection efficiency of our experimental arrangement, which appeared to be $\gtrsim$ 90%. Measurements of the net negative current produced in the cell ($= i_{slow\ -} - i_{slow\ +}$) equaled the measured loss of He^- due to attenuation to within ± 10%. Cross sections for the production of positive target ions were calculated from the measured values of $i_{slow\ +}$, and are given in Table III, along with the σ_{-10} cross sections.

The σ_{-10} cross sections presented in Figures 4 and 5 are large, approximately a factor of two greater than the corresponding cross sections for H^- in He, Ar, H_2, and O_2.[60] With the exception of the O_2 and NO results, the cross sections are relatively constant over the energy range investigated. Below 1 keV, both the O_2 and NO cross sections rise rapidly with decreasing energy, reaching 58 $Å^2$ for NO at 500 eV. Similar behavior has been seen in both the $H^- + O_2$ and $H^- + NO$ collisional detachment results.[60-62] For those systems, it was shown that most of the increase in the total cross section is attributable to a rise in the charge-transfer probability.[60,62] It seems likely that the same mechanism is responsible for the observed incease here. Both O_2 and NO have stable negative ions, and the reactions,

$$He^- (^4P) + O_2(^3\Sigma) \rightarrow He(^3S) + O_2^- (^2\Pi) + 0.36\ eV \qquad (11)$$

and

$$He^- (^4P) + NO\ (^2\Pi) \rightarrow He\ (^3S) + NO^-\ (^3\Sigma) + 0.04\ eV \qquad (12)$$

are energetically allowed.

The cross sections for target ionization given in Table III comprise between 15 and 30% of the corresponding σ_{-10} cross sections for Ar and O_2. It is interesting to note that there is very little He target ionization as expected since the Penning channel is not available. Since the 2p electron in the He^- (1s2s2p) ^4P produces additional shielding of the 1s core relative to He^* (1s2s) 2^3S, cross sections for Penning ionization by He^* 2^3S should represent an approximate upper bound for these target ionization cross sections. Measured total deexcitation cross sections of He^* 2^3S by Ar determined by Moseley et al.[63] and the Penning ionization cross sections calculated by Olson[64] are about a factor of two larger than our measured target ionization cross sections.

We have also applied the Bates and Walker classical impulse approximation method to calculate σ_{-10} cross sections down to 500 eV. Calculated values are included in Table III. In general, agreement for H_2 is good; however, for both He and Ar the calculated values are lower by up to an order of magnitude at the lowest energy. It seems clear that at these low energies, this simple treatment is no longer applicable.

5. CONCLUSIONS

The properties and interactions of He^- have been reviewed, with particular attention to recent photodetachment and collisional detachment cross section measurements. The small electron binding energy and the large electronic excitation of the metastable He^- ion are seen to give rise to distinct and interesting behavior. Moreover, since He^- is a simple three electron atom, it provides a good test system for theoretical calculations on negative ions in general and doubly excited ions in particular. One area

requiring additional theoretical attention is the description of the low energy collisional detachment processes, including the contributions due to target ionization.

ACKNOWLEDGEMENTS

The He^- photodetachment studies described here were originally proposed by Dr. J. R. Peterson, and done in collaboration with him and Dr. R. V. Hodges. The collisonal detachment work was done in association with Drs. K. T. Gillen and R. V. Hodges. In addition to acknowledging the contributions of these colleagues, the author would like to thank Mr. Ralph L. Leon for his assistance in designing and maintaining the scattering apparatus. This work was supported by the Office of Naval Research and the National Science Foundation.

REFERENCES

1. J. W. Hiby, Ann. Phys. Leipzig 34, 473 (1939).

2. Ta-You Wu, Phil. Mag. 22, 837 (1936).

3. E. Holøien and J. Midtdal, Proc. Phys. Soc. (London) A68, 815 (1955).

4. E. Holøien, Arch. Math. Naturv. 51, 81 (1951).

5. V. M. Dukel'skii, V. V. Afrosimov, and N. V. Fedorenko, JETP 3, 764 (1956).

6. P. M. Windham, P. J. Joseph, and J. A. Weinman, Phys. Rev. 109, 1193 (1958).

7. G. J. Lockwood, H. F. Helbig, and E. Everhart, Phys. Rev. 132, 2078 (1963).

8. T. Jorgensen, Jr., C. E. Kuyatt, W. W. Lang, D. C. Lorents, and C. A. Sautter, Phys. Rev. 140, A1481 (1965).

9. A. Papkow and G. J. Steiser, Z. Naturf. 21a, 1048 (1966).

10. B. L. Donnally and G. Thoeming, Phys. Rev. 159, 87 (1967).

11. Ya. M. Fosel', V. A. Ankudinov, and D. V. Philipenko, JETP 11, 18 (1960).

12. L. E. Collins and P. T. Stroud, Proc. Phys. Soc. A90, 641 (1967).

13. H. B. Gilbody, R. Browning, K. F. Dunn, and A. I. McIntosh, J. Phys. B 2, 465 (1969); H. B. Gilbody, K. F. Dunn, and R. Browning, 3, L19 (1970).

14. R. A. Baragiola and E. R. Salvatelli, J. Phys. B 8, 382 (1975).

15. K. F. Dunn, B. J. Gilmore, F. R. Simpson, and H. B. Gilbody, J. Phys. B 11, 1797 (1978).

16. J. R. Peterson and D. C. Lorents, Phys. Rev. 182, 152 (1969).

17. C. Reynaud, J. Pommier, Vu Ngoc Tuan, and M. Barat, Phys. Rev. Lett. 43, 579 (1979).

18. A. V. Bunge and C. F. Bunge, Phys. Rev. A 19, 452 (1979).

19. B. Brehm, M. A. Gusinow, and J. L. Hall, Phys. Rev. Lett. 737 (1967).

20. E. Holøien and J. Midtdal, Proc. Phys. Soc. A90, 883 (1967).

21. E. Holøien and S. Geltman, Phys. Rev. 153, 81 (1967).

22. J. L. Pietenpol, Phys. Rev. Lett. 7, 64 (1961).

23. S. T. Manson, Phys. Rev. 145, 35 (1966).

24. C. Laughlin and A. L. Stewart, J. Phys. B 1, 151 (1963).

25. G. N. Estberg and R. W. LaBahn, Phys. Lett. 28A, 420 (1968).

26. D. J. Nicholas, C. W. Trowbridge, and W. D. Allen, Phys. Rev. 167, 38 (1968).

27. L. M. Blau, R. Novick, and D. Weinflash, Phys. Rev. Lett. 24, 1268 (1970).

28. R. Novick and D. Weinflash, in "Precision Measurements and Fundamental Constants" (Proceedings of the International Conference at Gaithersburg, Md., 1970), edited by D. N. Langenberg and B. N. Taylor, National Bureau of Standards Special Publication No. 343 (U.S. GPO, Washington, D.C., 1971), pp. 403-410.

29. F. R. Simpson, R. Browning, and H. B. Gilbody, J. Phys. B 4, 106 (1971).

30. R. N. Compton, G. D. Alton, A. D. Williamson, and A. E. Carter, Abstracts of papers, XIth International Conference on the Physics of Electronic and Atomic Collisions (Kyoto, Japan), p. 68 (1979).

31. G. N. Estberg and R. W. LaBahn, Phys. Rev. Lett. 24, 1265 (1970).

32. D. L. Mader and R. Novick, Phys. Rev. Lett. 29, 199 (1972).

33. R. H. Neynaber and D. G. Magnuson, J. Chem. Phys. 65, 5239 (1976); R. H. Neynaber and S. Y. Tang, Chem. Phys. Lett. 65, 150 (1979).

34. M. J. Coggiola, T. D. Gaily, K. T. Gillen, and J. R. Peterson, J. Chem. Phys. 70, 2576 (1979); T. D. Gaily, M. J. Coggiola, J. R. Peterson, and K. T. Gillen, Rev. Sci. Instru. 51, 1168 (1980).

35. See for example: H. Hotop and W. C. Lineberger, J. Phys. Chem. Data 4, 539 (1975).

36. R. V. Hodges, M. J. Coggiola, and J. R. Peterson, Abstracts of 7th International Conference on Atomic Physics, Massachusetts Institute of Technology, Cambridge, MA (1980), p. 180; R. V. Hodges, M. J. Coggiola, and J. R. Peterson, Phys. Rev. A 23, 59 (1981).

37. R. N. Compton, G. D. Alton, and D. J. Pegg, J. Phys. B. 13, L651 (1980).

38. H. Hotop, T. A. Patterson, and W. C. Lineberger, Phys. Rev. A 8, 762 (1973).

39. A. U. Hazi and K. Reed, unpublished.

40. U. I. Safronova and V. S. Senashenko, Phys. Lett. 55A, 401 (1976).

41. A. V. Bunge and C. F. Bunge, unpublished.

42. R. S. Oberoi and R. K. Nesbet, Phys. Rev. A 8, 2969 (1973).

43. For a review of negative ion collisional detachment, see J. S. Risley in "Electronic and Atomic Collisions", Proceedings of the XIth International Conference on the Physics of Electronic and Atomic Collisions, Invited Papers and Progress Reports, Edited by N. Oda and K. Takayanagi (North Holland Publishing Co., Amsterdam 1980) p. 619.

44. J. Heinemein, P. Hvelplund, and F. R. Simpson, J. Phys. B 8, 1880 (1975); 9, 2669 (1976).

45. F. R. Simpson and H. B. Gilbody, J. Phys. B 5, 1959 (1972).

46. H. B. Gilbody, K. F. Dunn, R. Browning, and C. J. Latimer, J. Phys. B 3, 1105 (1970).

47. E. H. Pedersen and P. Hvelplund, J. Phys. B 6, 2600 (1973).

48. B. L. Donnally and W. Sawyer, Phys. Rev. Lett. 15, 439 (1965).

49. B. Donnally, W. Raith, and R. Beckert, Phys. Rev. Lett. 20, 575 (1968).

50. R. H. Hughes and H. Kisner, Phys. Rev. A 5, 2108 (1972).

51. E. H. Pedersen, F. R. Simpson, and P. Hvelplund, Phys. Rev. A 11, 516 (1975).

52. E. H. Pedersen, Phys. Rev. A 15, 53 (1977).

53. D. R. Bates and J. C. G. Walker, Planet. Space Sci. 14, 1367 (1966); Proc. Phys. Soc. A 90, 333 (1967).

54. D. R. Bates, V. Dose, and N. A. Young, J. Phys. B 2, 930 (1969).

55. R. Snyder, J. Phys. B 6, L8 (1963).

56. R. V. Hodges, M. J. Coggiola, and K. T. Gillen, to be published.

57. F. L. Eisele and S. W. Nagy, J. Chem. Phys. 65, 752 (1976).

58. R. Hegenberg, T. Stefansson, and M. T. Elford, J. Phys. B 11, 133 (1978).

59. G. Ryding, A. B. Wittkower, and P. H. Rose, Phys. Rev. 174, 149 (1968).

60. J. S. Risley and R. Geballe, Phys. Rev. A 9, 2485 (1974).

61. W. R. Snow, R. D. Rundel, and R. Geballe, Phys. Rev. 178, 228 (1969).

62. D. V. Pilipenko, V. A. Gusev, and Ya. M. Fogel', JETP 22, 965 (1966).

63. J. T. Moseley, J. R. Peterson, D. C. Lorents, and M. Hollstein, Phys. Rev. A 6, 1025 (1972).

64. R. E. Olson, Phys. Rev. A 6, 1031 (1972).

TABLE I Experimental Cross Sections for He^- Formation by Charge-Transfer of He^+ with Various Targets

Projectile	Energy (keV)	Target	Reported Cross Section (cm^2)	Reference
He^+	15-175	Ne, Ar, Kr	σ_{1-1} (Kr, 65 keV) = 1.5×10^{-19}	5
	15-20	H_2	σ_{1-1} (H_2, 17.5 keV) = 1×10^{-1}	6
	12-22	He	---	7
	50-200	He, H_2, N_2, O_2, Ar	σ_{0-1}(H_2, 150 keV) = 1.0×10^{-19}	8
	20-70	H_2, Kr, Xe, CO_2	σ_{1-1} (H_2, 70 keV) = 1.5×10^{-19}	9
	1-3	Cs	---	10
He	10-50	Ne, Ar, Kr, Xe	σ_{0-1} (Xe, 50 keV) = 2.0×10^{-19}	11
	80-200	H_2	---	12
	80-200	H_2	σ_{0-1} (H_2, 100 keV) = 5.4×10^{-18}	13
	20-40	Pb, Mg	σ_{0-1} (Mg, 40 keV) = 2.5×10^{-18}	14
	200	H_2	σ_{0-1} (H_2, 200 keV) = 1.1×10^{-18} (2^1S) 2.0×10^{-18} (2^3S)	15

TABLE II Absolute He^- (^4P) Photodetachment Cross Sections

λ (nm)	Laser	σ (10^{-17} cm^2)
10741	CO_2 - P(34)	11.8
10275	CO_2 - R(16)	11.4
9657	CO_2 - P(32)	12.3
9282	CO_2 - R(18)	12.0
1060	Nd:YAG	3.9
752.5	Kr^+	4.7
647.1	Kr^+	3.3
568.2	Kr^+	2.5
530.9	Kr^+	1.8
514.5	Ar^+	2.0
488.0	Ar^+	1.3
457.9	Ar^+	3.0
413.1	Kr^+	1.3
380.0	XeCl + BBQ	1.5
308.0	XeCl	0.8

TABLE III He^- Collisional Detachment Cross Sections for He, Ar, and O_2, Including Target Ionization and Calculated Cross Sections

Target	Energy (keV)	Cross Sections		
		Total destruction	Slow ion	Calc.
He	1.0	14.0 ± 1.3	< 0.3	6.4
	2.0	15.6 ± 1.3	< 0.6 ± 0.1	7.2
Ar	1.0	12.5 ± 0.6	2.3 ± 0.7	2.4
	1.5	12.1 ± 0.6	3.6 ± 0.4	2.6
	2.0	12.1 ± 0.6	3.8 ± 0.4	2.7
O_2	1.0	26.3 ± 1.2	4.0 ± 1.6	6.2
	2.0	24.1 ± 1.2	6.3 ± 0.7	6.3

FIGURE CAPTIONS

Fig. 1. Schematic diagram of the interaction region used for the He^- photodetachment experiment.

Fig. 2. Photodetachment cross section as a function of total energy relative to He (^1S_o) (lower scale) and photon wavelength (upper scale).
(•) results of Hodges, Coggiola, and Peterson, ref. 36.
(Δ) results of Compton, Alton, nd Pegg, ref. 37.

Fig. 3. Schematic diagram of the interaction region used for the He^- collisional detachment experiments. Not shown is the slow collector plate inside the scattering cell.

Fig. 4. Collisional detachment total cross sections for He^- on He, Ne, and Ar from 500 eV to 4 keV. The solid points at 4 keV are the data of Simpson and Gilbody, ref. 45.

Fig. 5. Collisional detachment total cross sections for He^- on NO, O_2, and H_2 from 500 eV to 4 keV. The solid point at 4 keV is the H_2 result of Simpson and Gilbody, ref. 45.

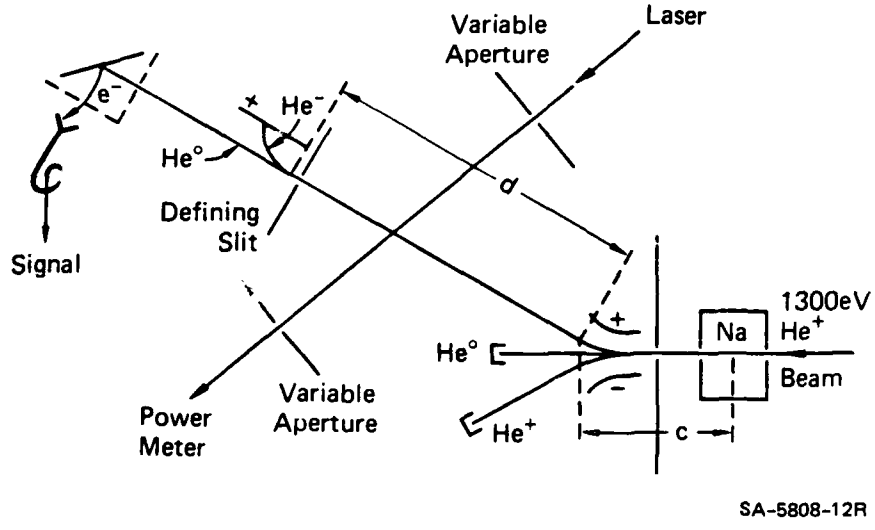

FIGURE 1 SCHEMATIC DIAGRAM OF THE INTERACTION REGION USED FOR THE He^- PHOTODETACHMENT EXPERIMENT

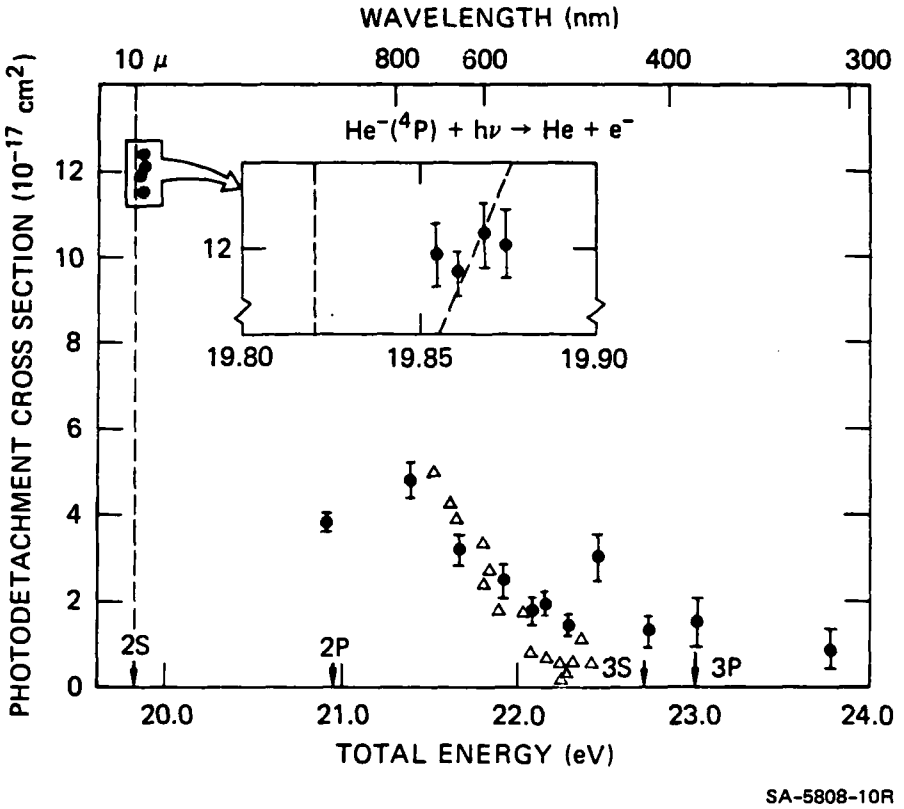

FIGURE 2 PHOTODETACHMENT CROSS SECTION AS A FUNCTION OF TOTAL ENERGY RELATIVE TO He (^1S_o) (lower scale) AND PHOTON WAVELENGTH (upper scale)

The arrows indicate outgoing excited He states. The inset shows the CO_2 laser data near 10 μm; the dashed line shows a $\nu(\nu - \nu_o)^{3/2}$ threshold curve "fitted" to the average of these data.

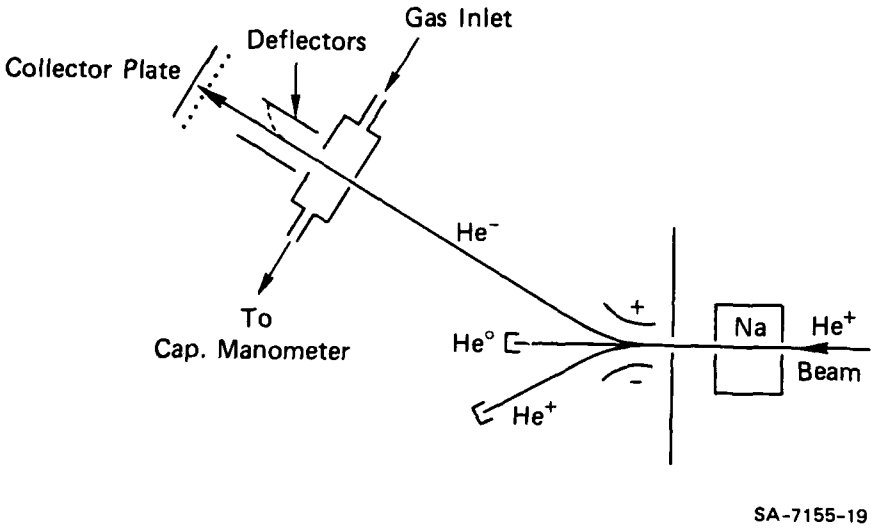
Gas Inlet
Deflectors
Collector Plate
He⁻
To
Cap. Manometer
+
Na
He⁺
He°
Beam
-
He⁺
SA-7155-19

FIGURE 3

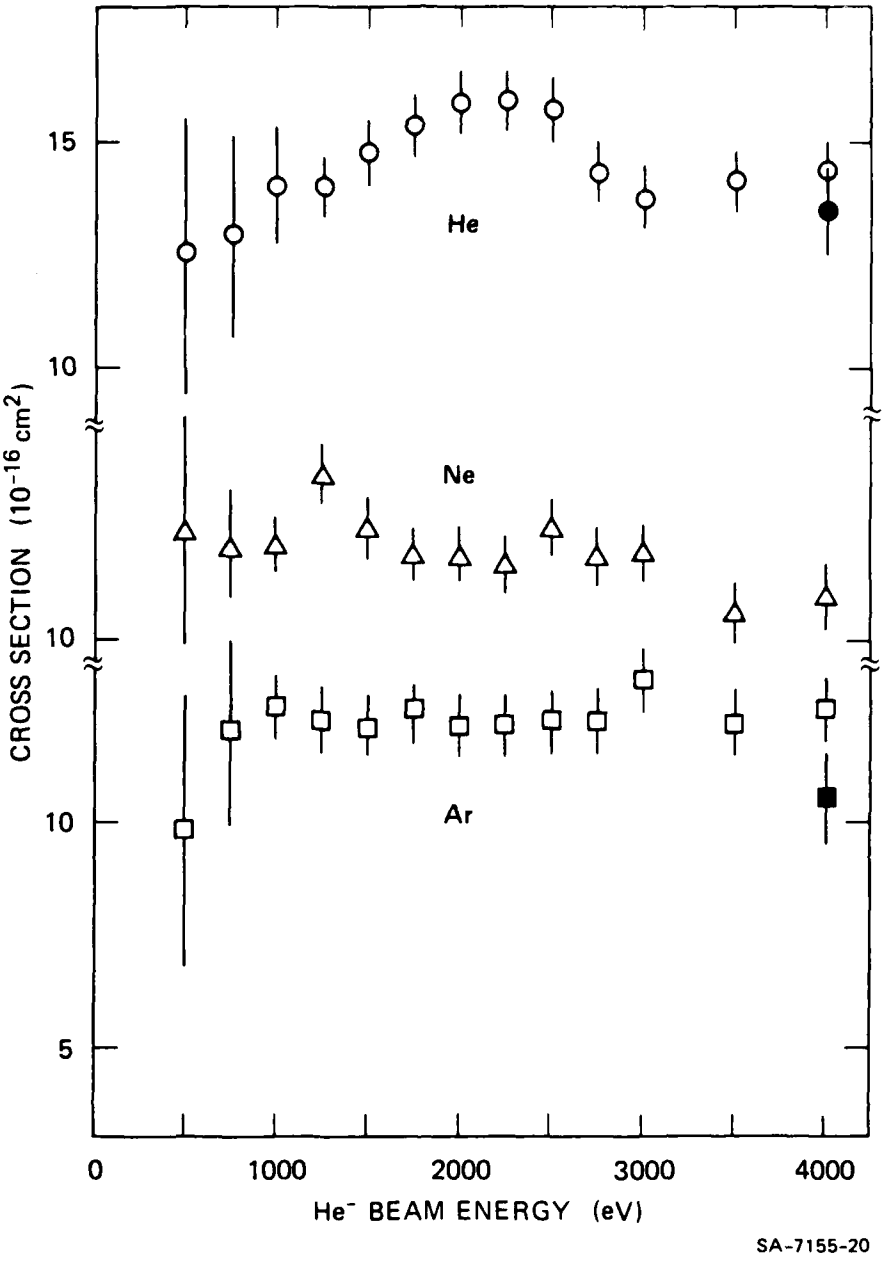
15
10
10
10
5
He
Ne
Ar
CROSS SECTION (10^{-16} cm^2)
0
1000
2000
3000
4000
He$^-$ BEAM ENERGY (eV)
SA-7155-20

FIGURE 4

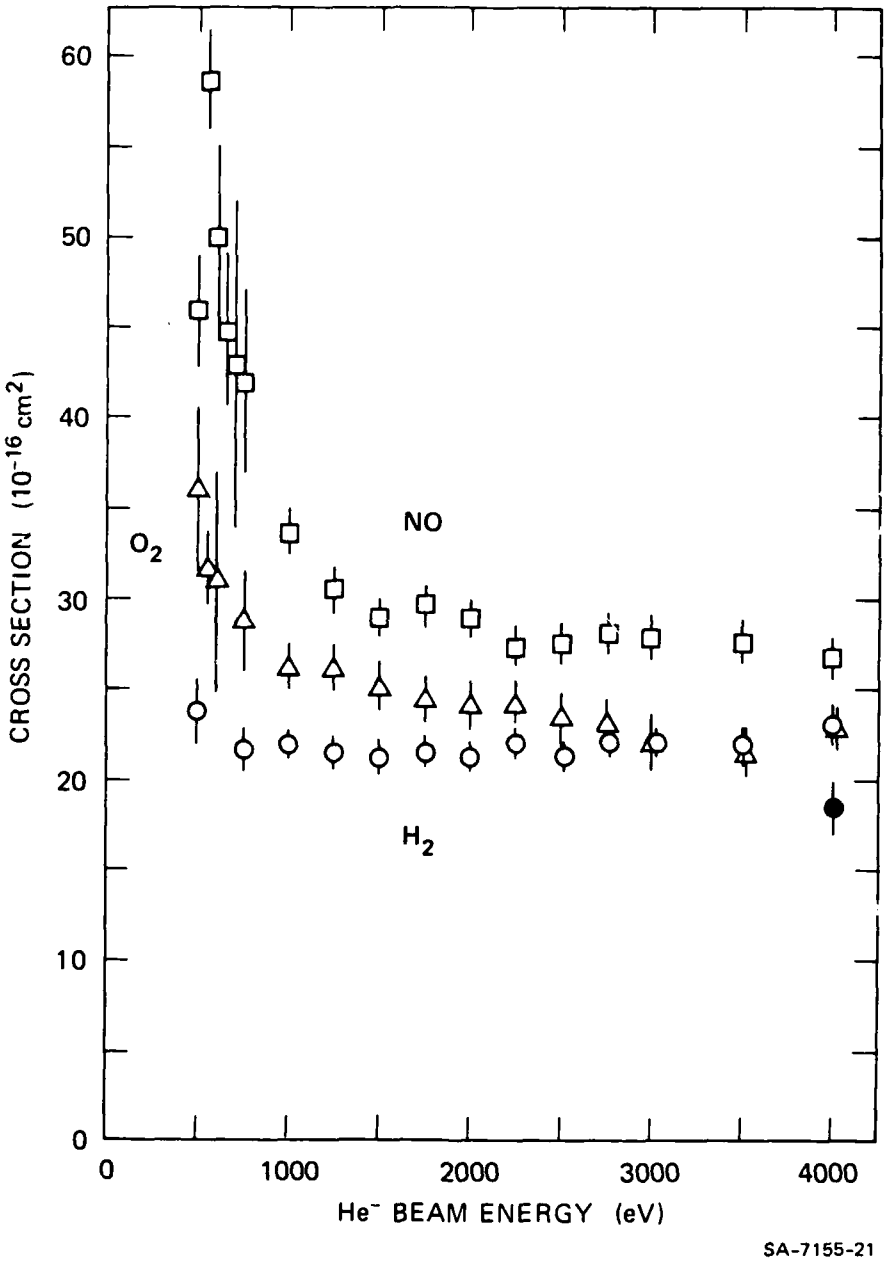
60
50
40
30
20
10
0
CROSS SECTION (10^{-16} cm^2)
O_2
NO
H_2
0
1000
2000
3000
4000
He$^-$ BEAM ENERGY (eV)
SA-7155-21

FIGURE 5

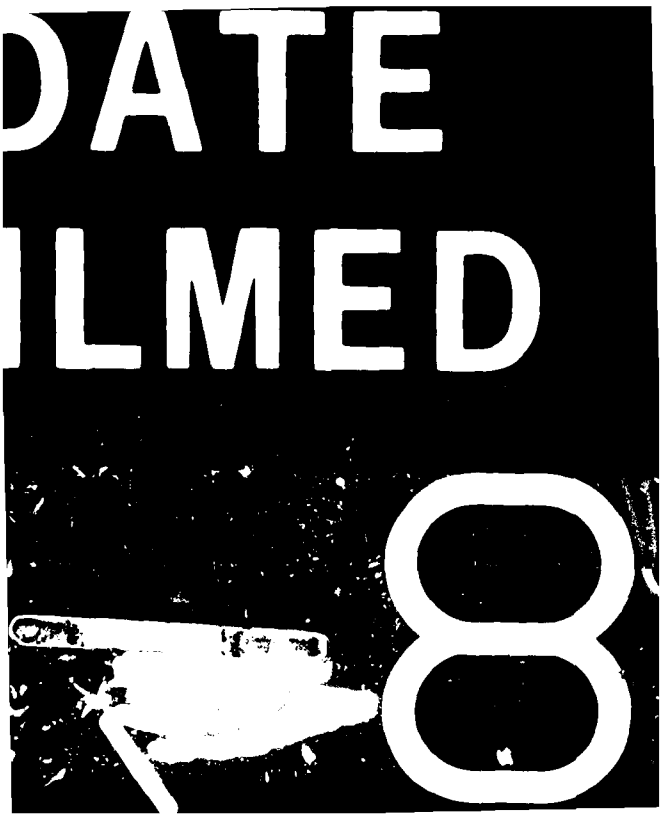
DATE
ILMED
8